INFORMAZIONI PERSONALI **SARA VIGANO'**

Sesso Femmina Data di Nascita 27/04/1983 Nazione ITALIA

POSIZIONE RICOPERTA DIRIGENTE MEDICO

ESPERIENZA PROFESSIONALE

Da Gennaio 2016 Radiologa Senologa

Fondazione IRCCS Ca' Granda - Ospedale Maggiore Policlinico, Milano

Radiologa senologa

Attività o Settore sanità

Da Giugno 2013 a Novembre 2013 HONORARY CLINICAL FELLOW

CAMBRIDGE UNIVERSITY HOSPITAL, UK

Clinical Fellow nella breast Unit (mammografie, biopsie, ecografie, screening, Risonanza magnetica); partecipazione multidisciplinary meeting

Attività o Settore SANITA'

Da Agosto 2014 a Luglio 2015 radiologo senologo

Fondazione IRCCS - Istituto Nazionale dei Tumori, Milano

Collaboratrice come radiologa senologa (mammografie, ecografia, biopsie); partecipazione allo studio multicentrico MRIB

Attività o Settore SANITA'

Da Agosto 2007 VOLONTARIA

stage volontario all'Hopital Saint Jean de Dieu, Afagnan, Togo, soprattutto nell'unità di ostetricia e ginecologia e di chirurgia generale

Attività o Settore SANITA'

Da Ottobre 2015 a Dicembre 2015 fellowship Breast Unit dell' AKH

FELLOWSHIP NELL'AMBITO DEL PROGRAMMA ESOR

Assistenza e partecipazione all'attività clinica dell'unità radiologica senologica

Attività o Settore sanità

ISTRUZIONE E FORMAZIONE

Da Ottobre 2015 a Dicembre 2015 Fellowship in Breast Radiology (programma ESOR)

Breast Unit dell' AKH - Allgemeines Krankenhaus der Stadt Wien - Medizinischer Universittscampus (Prof. Dr. Thomas Helbich)

Da Giugno 2013 a Novembre 2013 HoHonorary Clinical fellowship in Cambridge University Hospital NHS Foundation Trust

Cambridge University Hospital NHS Foundation Trust, Cambridge, UK (Prof. F.J. Gilbert e M. Wallis)

Da Ottobre 2012 EUSOBI Breast MRI Training Course 2012, Barcelona

ISTRUZIONE E FORMAZIONE

Da Giugno 2009 a Luglio 2014 Specializzazione in Radiodiagnostica

Scuola di specializzazione di Radiodiagnostica di Milano

discussione di tesi sperimentale "RM quantitativa per la predizione della risposta alla chemioterapia neoadiuvante del tumore mammario (Relatore Prof G. Cornalba, Correlatore Prof. F.Sardanelli)

Da Marzo 2009 iscrizione all'Albo Professionale dei Medici Chirurghi ed Odontoiatri di Milano

Ordine dei Medici Chirurghi ed Odontoiatri di Milano

Da Febbraio 2009 Abilitazione alla professione medica

l'Università Statale degli Studi di Milano

Da Ottobre 2008 Laurea in MEDICINA E CHIRURGIA

Università Statale degli Studi di Milano

COMPETENZE PERSONALI

Lingua madre Italiano

Altre lingue

	COMPRENSIONE		PARLATO		PRODUZIONE SCRITTA
	Ascolto	Lettura	Interazione	Produzione orale	
Inglese	B2	B2	B2	B2	B1
Tedesco	A2	A2	A2	A2	A2

Certificato: SPRACHENZENTRUM Wien, Level a2 (13/1

Livelli: A 1/2 Livello Base - B 1/2 Livello Intermedio - C 1/2 Livello Avanzato

Quadro Comune Europeo di Riferimento delle Lingue

Competenze informatiche 10/04/2003 ECDL (European Computer Driving Licence) START (modules: using the computer and managing files; Word processing; Spreadshit; Internet information and communication)

Patente di guida B

ALLEGATI

vigano.pdf
sconfienza.pdf
wash out.pdf
screening women at ir.pdf
trecate 2012 jena.pdf
poster ECR 2012.pdf
pacei.pdf

Dati personali Autorizzo il trattamento dei miei dati personali ai sensi del Decreto Legislativo 30 giugno 2003, n, 196 'Codice in materia di protezione dei dati personali'.

Clinical Radiology 68 (2013) e624–e628

Contents lists available at SciVerse ScienceDirect

Clinical Radiology

journal homepage: www.clinicalradiologyonline.net

Prevalence of cerebral aneurysms in patients treated for left cardiac myxoma: A prospective study

S. Viganò [a], G.D.E. Papini [b], B. Cotticelli [b], L. Valvassori [c], A. Frigiola [d], L. Menicanti [d], G. Di Leo [b,*], F. Sardanelli [b,e]

[a] *Scuola di Specializzazione in Radiodiagnostica, Università degli Studi di Milano, Milano, Italy*
[b] *Unità di Radiologia, IRCCS Policlinico San Donato, San Donato Milanese, Italy*
[c] *Dipartmento di Neuroradiologia, Azienda Ospedaliera Niguarda Ca' Granda, Milano, Italy*
[d] *Unità di Cardiochirurgia, IRCCS Policlinico San Donato, San Donato Milanese, Italy*
[e] *Dipartimento di Scienze Biomediche per la Salute, Università degli Studi di Milano, San Donato Milanese, Italy*

ARTICLE INFORMATION

Article history:
Received 22 March 2013
Received in revised form
3 June 2013
Accepted 11 June 2013

AIM: To estimate the prevalence of cerebral aneurysms in patients previously treated for left cardiac myxoma (LCM).

MATERIALS AND METHODS: This prospective institutional review board-approved study included patients treated for LCM. All patients treated at our institution (IRCCS Policlinico San Donato, Italy) were telephoned and those enrolled underwent unenhanced brain magnetic resonance imaging (MRI) using sagittal T1-weighted turbo spin-echo (TSE); axial T2-weighted TSE; axial fluid-attenuated inversion-recovery; axial echo-planar diffusion-weighted; and three-dimensional time-of-flight angiographic sequences.

RESULTS: Seventy-six patients were telephoned, and data regarding their clinical history since tumor resection were obtained for 49 patients (64%). Four of the 49 (8%) patients were deceased, one due to a cerebral hemorrhage from a ruptured cerebral aneurysm 8 years after tumor resection. One patient had a pacemaker preventing MRI. Of the remaining 44 patients, 31 refused MRI and 13 were enrolled (10 females; mean age 64 years). Three of the 13 (23%; two females; 59–78 years) were diagnosed with a cerebral aneurysm, from 2 mm to 4–5 mm in diameter, involving the right middle cerebral artery ($n = 2$) or the right internal carotid artery ($n = 1$). Including the deceased patient, the resulting prevalence was 4/14 (29%).

CONCLUSION: From this preliminary study, one-third of patients treated for LCM may present with a cerebral aneurysm. Longitudinal large studies are needed to further clarify this matter.

Introduction

Cardiac myxoma is the most common primary cardiac tumour[1] with an autopsy-estimated prevalence ranging 0.0017–0.19%.[2] It is mainly located in the left atrium (75–80%). Age of onset is very variable, ranging from childhood to elderly,[3–5] with a higher prevalence in female patients (57–78%).[5–8] Other than cardiac and general symptoms, patients may present embolic and neurological symptoms, mainly involving the central nervous system, reported in up to 26% of patients,[3,5,6,8] the most frequent being ischaemic events.[6,9,10]

Further acute or delayed neurological events include development of intracranial aneurysms and intracranial or subarachnoid haemorrhages.[9,10] Up to 17% of patients with

* Guarantor and correspondent: G. Di Leo, Unità di Radiologia, IRCCS Policlinico San Donato, Piazza E. Malan, 20097 San Donato Milanese, Italy. Tel.: +39 02 52774468; fax: +39 02 52774925.
E-mail address: gianni.dileo77@gmail.com (G. Di Leo).

0009-9260/$ – see front matter © 2013 The Royal College of Radiologists. Published by Elsevier Ltd. All rights reserved.
http://dx.doi.org/10.1016/j.crad.2013.06.010

neurological symptoms were reported to have a cerebral bleed,[9] possibly due to ruptured cerebral aneurysms. Myxoma-related cerebral aneurysms were first reported by Marchand in 1894,[11] and follow-up using cerebral imaging after myxoma resection for the development of myxoma-related aneurysms has been recommended.[12] Nevertheless, knowledge about this association derives only from case reports and retrospective studies.[12–14]

Thus, despite great knowledge of acute neurological complications, little is known about delayed neurological events, especially cerebral aneurysms. The pathogenesis is not fully understood and the natural history is unclear. Various authors have described cases with stable aneurysms[14–18] or progressively enlarging or newly developing aneurysms.[14,19,20] Latency between myxoma resection and the diagnosis of cerebral aneurysms is very variable. They may be diagnosed before cardiac surgery, but also many years after.[14,21,22] Some authors have shown that the development of cerebral aneurysms can occur after myxoma resection.[20,23,24] Although surgical removal of the primary cardiac neoplasm may prevent early neurological embolic events, late events, such as cerebral aneurysm formation, cannot be excluded.[19,21] Moreover, a standardized therapy has not been established for myxoma-related cerebral aneurysms, and there is no general consensus on their management. The prevalence of cerebral aneurysms in patients treated for left cardiac myxoma has been reported to be higher when compared to the general population; however, the real prevalence of cerebral aneurysms in patients treated for cardiac myxoma is unknown and no prospective studies have been conducted.[25] Thus, the aim of the present study was to prospectively assess the prevalence of cerebral aneurysms in patients previously treated for left cardiac myxoma.

Materials and methods

This prospective study was approved by the local ethics committee. The inclusion criterion was previous surgical excision of left cardiac myxoma. An attempt was made to telephone patients surgically treated for left cardiac myxoma at our institution (IRCCS Policlinico San Donato, Italy) between 1990 and 2009. Clinical data regarding neurovascular events were collected. Exclusion criteria were site of myxoma other than left cardiac chambers; contraindication to magnetic resonance imaging (MRI); and any status precluding the ability to sign the informed consent.

After signing the informed consent form, patients underwent the mini mental state examination[26] in order to evaluate their cognitive status. This score was normalized for education level.

MRI protocol and analysis

Patients enrolled in the study underwent 1.5 T unenhanced brain MRI (Magnetom Sonata Maestro Class, Siemens Medical Solution, Erlangen, Germany) with the following sequences: (a) three-plain gradient-echo localizer; (b) sagittal T1-weighted turbo spin-echo (repetition time 635 ms, echo time 17 ms, section thickness 5 mm, field of view 250 × 250 mm, matrix 256 × 256, acquisition time 2 min and 47 s); (c) axial T2-weighted turbo spin-echo (repetition time 4760 ms, echo time 94 ms, section thickness 5 mm, field of view 230 × 201 mm, matrix 256 × 256, acquisition time 2 min and 52 s); (d) axial fluid-attenuated inversion-recovery (repetition time 8650 ms, echo time 109 ms, inversion time 2500 ms, section thickness 5 mm, field of view 230 × 201 mm, matrix 256 × 256, acquisition time 3 min and 28 s); (e) axial echo-planar diffusion weighted sequences (b values = 0, 500, and 1000 s/mm^2; recovery time 3900 ms, echo time 87 ms, section thickness 5 mm, field of view 250 × 250 mm, matrix 128 × 128, acquisition time 1 min and 34 s); (f) three-dimensional time-of-flight angiographic sequence with multiplanar and three-dimensional (3D) maximum-intensity projection (MIP) reconstructions (recovery time 34 ms, echo time 4.45 ms, section thickness 0.8 mm, field of view 250 × 187.5 mm, matrix 384 × 384, acquisition time 6 min and 55 s). MRI images were evaluated in consensus by two neuroradiologists with 3 and 12 years of experience.

Work-up of MRI findings

In the case of detection of MRI findings suspicious for cerebral aneurysms, the patient was referred to interventional neuroradiology to evaluate the possibility of further diagnostic imaging and therapeutic approach.

Statistical analysis

Demographics are presented as means and standard deviations. The prevalence of cerebral aneurysms was calculated as the number of patients diagnosed with the disease on cerebral MRI divided by the number of patients who underwent cerebral MRI, with 95% confidence intervals (CI) calculated according the binomial distribution.

Results

Patient population

From 1990 to 2009, 84 patients underwent surgery for cardiac myxoma. Eight patients were excluded: five had a cardiac myxoma in right cardiac chambers; in three patients the final pathological diagnosis was not available (two patients died during the intervention). Thus, 76 patients were eligible for the study. The mean age at the time of tumor resection was 60 ± 13 years (range 23–83 years), with a median age of 62 years. Forty-seven were women (63%). For 49 of these 76 patients (64%), information regarding current status and clinical history since tumor resection was obtained by telephone. For four of 49 cases (8%), the person answering the call stated that the patient was deceased; one death was caused by cerebral hemorrhage due to a ruptured cerebral aneurysm approximately 8 years after tumor resection. Moreover, one patient had a pacemaker, which contraindicated MRI.

Enrollment and MRI results

Of the remaining 44 patients, 31 (70%) declined and 13 (30%, 10 women and three men, aged 64 ± 10 years; range 45–79 years) were enrolled and underwent brain MRI. No cognitive impairment was found at the mini mental state examination, the score ranging between 25 and 30. Out of 13 patients, three (23%) were diagnosed with a cerebral aneurysm on MRI: (1) one female patient of 59 years of age, who underwent surgery for cardiac myxoma at 49 years, was diagnosed with a berry aneurysm of 2 mm in diameter in the M1 tract of the right middle cerebral artery, near its bifurcation (Fig 1); this patient reported episodes of vertigo and headache; (2) one female patient of 66 years, who underwent surgery for cardiac myxoma at 62 years, was diagnosed with a small saccular aneurysm of 3–4 mm in diameter in the proximal M1 tract of the right middle cerebral artery (Fig 2); this patient reported headache; (3) one male patient of 78 years of age, who underwent surgery for cardiac myxoma at 68 years, was diagnosed with a saccular aneurysm of 4–5 mm in diameter in the C4 tract (according to Fischer classification[27]) of the right internal carotid artery, arising from the lateral side of the vessel (Fig 3); this patient reported no neurological symptoms. Moreover, MRI showed a right cerebellar lacunar infarction in the first patient and multiple lacunar infarcts in basal ganglia in the third patient.

Among the remaining 10 patients, MRI showed anatomical variants of the P1 tract of the cerebral posterior artery in two patients and hypoplasia of the A1 tract of the right anterior cerebral artery in another patient; small lacunar infarcts were found in the basal ganglia, left parietal

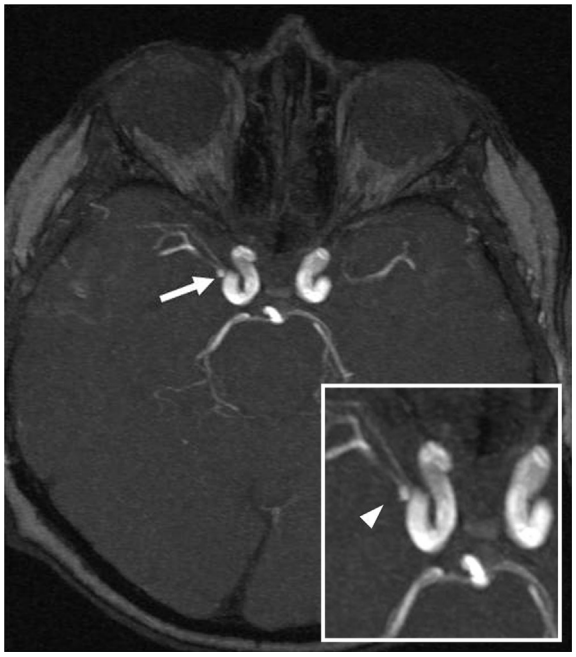

Figure 2 Female patient, 66 years old, underwent surgery for cardiac myxoma at 62 years. 3D time-of-flight sequences from the cerebral MRI showed a small, 3–4 mm diameter, saccular aneurysm in the proximal M1 tract of the right middle cerebral artery. This patient reported headache.

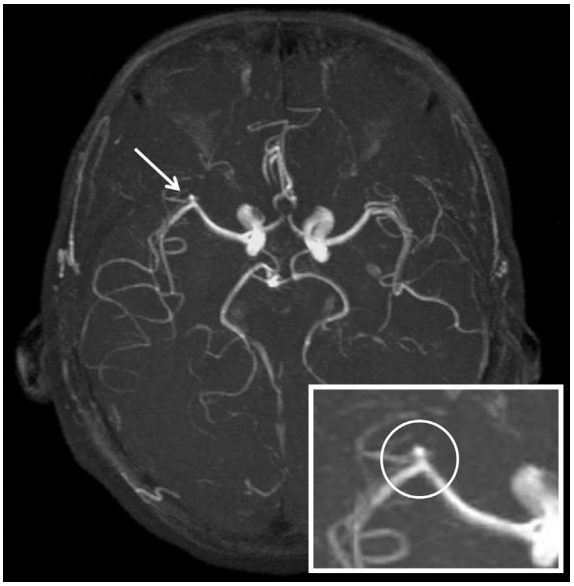

Figure 1 Female patient, 59 years old, underwent surgery for cardiac myxoma at 49 years. An MIP reconstruction from the 3D time-of-flight sequences disclosed a 2 mm diameter berry aneurysm (arrow) on the M1 tract of the right middle cerebral artery, near the bifurcation and the origin of the fronto-orbital artery. This patient reported headache and vertigo.

Figure 3 Male patient of 78 years of age, who underwent surgery for cardiac myxoma at 68 years, was diagnosed with a large, 4–5 mm, saccular aneurysm in the C4 tract (according to Fischer) of the right internal carotid artery, arising from the lateral side of the vessel, which can be seen both on 3D time-of-flight sequences and MIP reconstruction. This patient reported no neurological symptoms.

lobe, ascendant gyrus of the right frontal lobe, and right cerebellum in three patients. One patient reported an episode of drop attack; the same patient was surgically treated for pituitary macroadenoma. The other nine patients did not report relevant neurological symptoms.

All the three patients diagnosed with cerebral aneurysm at MRI, were evaluated by experienced interventional neuroradiologists who confirmed the diagnosis. None of the patients underwent digital subtraction angiography, and diagnostic follow-up was advised within 2–3 years for all patients.

The prevalence of cerebral aneurysms in the present group of patients previously treated for left cardiac myxoma who underwent brain MRI was three of 13 patients (23%; 95% CI 5–54%). If the case of the patient who died from ruptured cerebral aneurysm was included, the prevalence of cerebral aneurysms becomes four of 14 patients (29%; 95% CI 8–58%).

Discussion

The aim of the present prospective study was to assess the prevalence of cerebral aneurysms in patients previously treated for left cardiac myxoma. Three patients were found to have cerebral aneurysms among the 13 patients who underwent MRI; one patient was reported to have died from a ruptured cerebral aneurysm. This produced an overall prevalence ranging from 23–29%. Cognitive function was normal in all these 13 patients, as expected.

Formation of myxoma-related cerebral aneurysms has been described and documented since 1894,[11] but current knowledge on this association derives only from case reports[13,15,18,19,21–23,25,28–31] and retrospective studies.[5,6,9,10,12–14] Standard of care was not established. Although cardiac surgery for removing the myxoma can eliminate early neurological symptoms, risk of delayed neurological events, such as cerebral aneurysms development, cannot be completely eliminated.[12,14,23]

The prevalence of myxoma-related cerebral aneurysms varies in previous studies, especially as no systematic investigation using neuroradiological imaging was undertaken. Lee et al.[10] reviewed 74 patients treated for cardiac myxoma and reported one patient with cerebral aneurysms and hemorrhage among nine patients presenting with neurological symptoms. Patients with neurological events underwent neuroimaging: the prevalence of cerebral aneurysms was 11% (1/9). Ekinci et al.[9] considered 113 patients treated for cardiac myxoma with neurological symptoms (six from their own centre and 107 from the literature). Cerebral aneurysms were reported in six patients at the time of myxoma diagnosis, giving a prevalence of 10% (11/113). Lee et al.[6] reported the prevalence of cerebral aneurysms was 2% (1/59) in patients treated for cardiac myxoma and 8% (1/13) among patients with cardiac myxoma and embolic signs. Interestingly, the case of cerebral aneurysms was not reported in a patient with brain emboli, but it was an incidental finding in a patient presenting with only systemic embolic symptoms. Pinede et al.[5] found three cases of cerebral aneurysms among 29 patients treated for cardiac myxoma with neurological symptoms (10%). Considering all of the 112 patients with cerebral aneurysms with and without neurological symptoms reviewed by the authors, the prevalence of cerebral aneurysms would be 3% (3/112). Tamulevičiūtė et al.[14] retrospectively matched two databases, one concerning 2246 patients with cerebral aneurysms and the other one concerning 40 patients treated for cardiac myxoma; a single patient was present in both databases.

Although there was a large confidence interval, the prevalence of myxoma-related cerebral aneurysms in the present study was higher than that previously reported, probably due to the aforementioned lack of systematic imaging evaluation in previous studies. In addition, cerebral aneurysms were prospectively sought using a protocol including magnetic resonance angiography (MRA), whereas other studies did not report using a standardized imaging protocol. Another explication is the selection of only left cardiac myxoma patients, which are reported to be more likely to embolize and promote aneurysm formation.[9]

Moreover, in the present study, the prevalence of cerebral aneurysms appears to be higher than that reported for the general population, ranging 2–6% according to study design and population as well as aneurysm characteristics.[32–36] Vlak et al.[32] reported a 3% prevalence of unruptured aneurysms in the general population (mean age 50 years) with a higher prevalence in females (6%). White and Wardlaw[33] reported a 4–6% prevalence of cerebral aneurysms in a population of >30-year-old patients, and Jeon et al.[34] described a prevalence of 5%. Horikoshi et al.[35] found incidental cerebral aneurysms at MRA in 3% of all patients. For adults without specific risk factors, Rinkel et al.[36] reported a prevalence of 2%, whereas it was found to be 4% in prospective autopsy studies, 4% in retrospective angiography studies, and 6% in prospective angiography studies.[36] Thus, the prevalence of unruptured myxoma-related cerebral aneurysms in the present study was substantially higher than that in the general population.

Although myxoma-related cerebral aneurysms were mainly reported to be multiple, fusiform, and located in distal arterial branches,[13,14] the aneurysms in the present study were unique, saccular, and located in the proximal tracts of the arteries. This would be due to the use of unenhanced MRI at 1.5 T, using a non-multicoil and relatively low-resolution protocol, potentially missing small peripheral cerebral aneurysms. However, the present results are consistent with previous studies, which reported saccular and central aneurysms as myxoma-related aneurysms despite being less frequent.[13,14,21] Li et al.[15] reported a case presenting with saccular and fusiform aneurysms, both proximal and distal. Yilmaz et al.[21] reported a patient with a giant aneurysm in the proximal tract of the middle cerebral artery, and a large saccular aneurysm in the circle of Willis' was described by Baikoussis et al.[28] Lee et al.[10] reported one patient with a 3 mm myxoma-related aneurysm of the left internal carotid artery. The three aneurysms found in the present series are consistent with these results. A similar reasoning holds for the right-sided location of the present

aneurysms, in agreement with previous findings and consistent with data on embolic strokes.[13]

The association between myxoma-related aneurysms and brain infarcts has been previously reported.[14] For patients who underwent left myxoma resection presenting with ischaemic stroke or transient ischaemic attack secondary prevention with anticoagulant or anti-platelets has been proposed.[9,37] In cases such as those, it has been claimed that there is a necessity to exclude cerebral aneurysms.[37] One of the present patients was reported to have had fatal ruptured cerebral aneurysm 8 years after myxoma resection. In fact, even though myxoma-related aneurysms can remain stable over years,[5,18,25,30] they may grow or rupture[10,13,14,19,31] up to 25 years later.[14,21,23] The three patients in the present study were treated conservatively with follow-up, as per previous recommendations.[5,18,25,30] However, the paucity of long-term follow-up in the literature should be reflected upon.

The present study has limitations. Apart from the above-mentioned non-high field, non-multicoil MRI technique, the sample size of patients who underwent MRI was small, thus limiting the extent of the data.

In conclusion, the present study prospectively showed a higher prevalence of cerebral aneurysms in patients treated for left cardiac myxoma, suggesting brain MRI to be appropriate in these patients. Transverse studies investigating the brain when cardiac myxoma is diagnosed and large longitudinal studies are needed to further clarify this matter.

References

1. Blondeau P. Primary cardiac tumors—French studies of 533 cases. *Thorac Cardiovasc Surg* 1990;**38**(Suppl. 2):192–5.
2. Reynen K. Cardiac myxomas. *N Engl J Med* 1995;**333**:1610–7.
3. Jelic J, Milicić D, Alfirević I, et al. Cardiac myxoma: diagnostic approach, surgical treatment and follow-up. A twenty years experience. *J Cardiovasc Surg (Torino)* 1996;**37**(Suppl. 1):113–7.
4. Aggarwal SK, Barik R, Sarma TC, et al. Clinical presentation and investigation findings in cardiac myxomas: new insights from the developing world. *Am Heart J* 2007;**154**:1102–7.
5. Pinede L, Duhaut P, Loire R. Clinical presentation of left atrial cardiac myxoma. A series of 112 consecutive cases. *Medicine (Baltimore)* 2001;**80**:159–72.
6. Lee SJ, Kim JH, Na CY, et al. Eleven years' experience with Korean cardiac myxoma patients: focus on embolic complications. *Cerebrovasc Dis* 2012;**33**:471–9.
7. Tasoglu I, Tutun U, Lafci G, et al. Primary cardiac myxomas: clinical experience and surgical results in 67 patients. *J Card Surg* 2009;**24**:256–9.
8. Garatti A, Nano G, Canziani A, et al. Surgical excision of cardiac myxomas: twenty years experience at a single institution. *Ann Thorac Surg* 2012;**93**:825–31.
9. Ekinci EI, Donnan GA. Neurological manifestations of cardiac myxoma: a review of the literature and report of cases. *Intern Med J* 2004;**34**:243–9.
10. Lee VH, Connolly HM, Brown Jr RD. Central nervous system manifestations of cardiac myxoma. *Arch Neurol* 2007;**64**:1115–20.
11. Marchand F. Zur kenntnis der embolie und thrombose der gerhirnarterien, zugleich ein beitrag zur casuistik der primaren herztumoren und der gekreuzten embolie. *Klin Wochenschr* 1894;**31**:1–5.
12. Stöllberger C, Finsterer J. Patients with cardiac myxoma require surveillance for myxoma-related cerebral aneurysms. *Eur J Neurol* 2008;**15**:e110–1.
13. Sabolek M, Bachus-Banaschak K, Bachus R, et al. Multiple cerebral aneurysms as delayed complication of left cardiac myxoma: a case report and review. *Acta Neurol Scand* 2005;**111**:345–50.
14. Tamulevičiūtė E, Taeshineetanakul P, Terbrugge K, et al. Myxomatous aneurysms: a case report and literature review. *Interv Neuroradiol* 2011;**17**:188–94.
15. Li Q, Shang H, Zhou D, et al. Repeated embolism and multiple aneurysms: central nervous system manifestations of cardiac myxoma. *Eur J Neurol* 2008;**15**:e112–3.
16. Herbst M, Wattjes MP, Urbach H, et al. Cerebral embolism from left atrial myxoma leading to cerebral and retinal aneurysms: a case report. *AJNR Am J Neuroradiol* 2005;**26**:666–9.
17. Roscher AA, Kato NS, Quan H, et al. Intra-atrial myxomas, clinical–pathologic correlation based on two case studies including historical review. *J Cardiovasc Surg (Torino)* 1996;**37**:131–7.
18. Ryou KS, Lee SH, Park SH, et al. Multiple fusiform myxomatous cerebral aneurysms in a patient with Carney complex. *J Neurosurg* 2008;**109**:318–20.
19. Eddleman CS, Gottardi-Littell NR, Bendok BR, et al. Rupture of cerebral myxomatous aneurysm months after resection of the primary cardiac tumor. *Neurocrit Care* 2010;**13**:252–5.
20. Furuya K, Sasaki T, Yoshimoto Y, et al. Histologically verified cerebral aneurysm formation secondary to embolism from cardiac myxoma. Case report. *J Neurosurg* 1995;**83**:170–3.
21. Yilmaz MB, Akin Y, Güray U, et al. Late recurrence of left atrial myxoma with multiple intracranial aneurysms. *J Cardiol* 2003;**87**:303–5.
22. Jean WC, Walski-Easton SM, Nussbaum ES. Multiple intracranial aneurysms as delayed complications of an atrial myxoma: case report. *Neurosurgery* 2001;**49**:200–2. discussion 202–3.
23. Hwang BJ, Connelly MM, Lev MH. Distinctive MR imaging appearance of hemorrhagic cerebral aneurysms associated with atrial myxoma. *AJR Am J Roentgenol* 2001;**177**:925–7.
24. Suzuki T, Nagai R, Yamazaki T, et al. Rapid growth of intracranial aneurysms secondary to cardiac myxoma. *Neurology* 1994;**44**:570–1.
25. Sedat J, Chau Y, Dunac A, et al. Multiple cerebral aneurysms caused by cardiac myxoma. A case report and present state of knowledge. *Interv Neuroradiol* 2007;**13**:179–84.
26. Folstein MF, Folstein SE, McHugh PR. "Mini-mental state". A practical method for grading the cognitive state of patients for the clinician. *J Psychiatr Res* 1975;**12**:189–98.
27. Bouthillier A, van Loveren HR, Keller JT. Segments of the internal carotid artery: a new classification. *Neurosurgery* 1996;**38**:425–32. discussion 432–433.
28. Baikoussis NG, Siminelakis SN, Kotsanti A, et al. Multiple cerebral mycotic aneurysms due to left atrial myxoma: are there any pitfalls for the cardiac surgeon? *Hellenic J Cardiol* 2011;**52**:466–8.
29. Oguz KK, Firat MM, Cila A. Fusiform aneurysms detected 5 years after removal of an atrial myxoma. *Neuroradiology* 2001;**43**:990–2.
30. Josephson SA, Johnston SC. Multiple stable fusiform intracranial aneurysms following atrial myxoma. *Neurology* 2005;**64**:526.
31. Rodriguez FJ, Brown RD, Mohr JP, et al. Embolic atrial myxoma with neoplastic aneurysm formation and haemorrhage: a diagnostic challenge. *Neuropathol Appl Neurobiol* 2006;**32**:213–6.
32. Vlak MH, Algra A, Brandenburg R, et al. Prevalence of unruptured intracranial aneurysms, with emphasis on sex, age, comorbidity, country, and time period: a systematic review and meta-analysis. *Lancet Neurol* 2011;**10**:626–36.
33. White PM, Wardlaw JM. Unruptured intracranial aneurysms. *J Neuroradiol* 2003;**30**:336–50.
34. Jeon TY, Jeon P, Kim KH. Prevalence of unruptured intracranial aneurysm on MR angiography. *Korean J Radiol* 2011;**12**:547–53.
35. Horikoshi T, Akiyama I, Yamagata Z, et al. Retrospective analysis of the prevalence of asymptomatic cerebral aneurysm in 4518 patients undergoing magnetic resonance angiography—when does cerebral aneurysm develop? *Neurol Med Chir (Tokyo)* 2002;**42**:105–12. discussion 113.
36. Rinkel GJ, Djibuti M, Algra A, et al. Prevalence and risk of rupture of intracranial aneurysms: a systematic review. *Stroke* 1998;**29**:251–6.
37. Nagy CD, Levy M, Mulhearn 4th TJ, et al. Safe and effective intravenous thrombolysis for acute ischemic stroke caused by left atrial myxoma. *J Stroke Cerebrovasc Dis* 2009;**18**:398–402.

European Journal of Radiology 81S1 (2012) S165–S170

Contents lists available at SciVerse ScienceDirect

European Journal of Radiology

journal homepage: www.elsevier.com/locate/ejrad

What is specific in hereditary breast cancer? High T2 signal intensity as a new semeiotic pattern?

Giovanna Trecate[a,*], Roberto Agresti[b], Laura Suman[a], Daniele Vergnaghi[a], Barbara Valeri[c], Monica Marchesini[a], Claudio Ferranti[a], Cristina Ferraris[b], Siranoush Manoukian[d], Gianfranco Scaperrotta[a], Sara Viganò[a], Pietro Panizza[a]

[a] Unit of Diagnostic Radiology "1", [b] Unit of Breast Surgery, [c] Unit of Pathology, [d] Department of Oncology-Medical Genetics, Fondazione IRCCS Istituto Nazionale dei Tumori, via G.Venezian 1, 20133 Milan, Italy

ARTICLE INFO

Keywords:
High T2 signal intensity
High speed of growth
Specific matrix in hereditary breast carcinomas

1. Objectives

Based on its spatial and contrast resolution and higher sensitivity in comparison with conventional imaging, Mammography (Mx) and Ultrasound (Us), Magnetic Resonance Imaging (MRI) has been included in screening protocols in patients at high risk to develop breast cancer. Stated some biologic and radiological differences between hereditary and sporadic cancer [1,2], the aim of our study was to analyze the MRI semeiotic patterns of hereditary tumour and to observe the eventual differences in comparison with sporadic neoplasm.

2. Methods

During 11 years, we enrolled 300 women at high genetic risk for breast cancer in a surveillance program, in the context of the multicentric study (HIBCRIT-1/2) coordinated by the Istituto Superiore di Sanità (Rome, Italy). Over this period we detected 44 breast tumours, one of which not evaluated with MRI because of claustrophobia, and compared them with the ones of 40 consecutive sporadic neoplasm that had been submitted to MRI examination at our Department. Morphologic and dynamic characteristics of both of these groups were analyzed. Informed consent was acquired for each patient.

3. Results

While we didn't observe any significant difference between morphologic or dynamic aspects, the surprising main semeiotic difference was related to the signal intensity on T2-weighted images that could not be considered as typical for cancer. If in fact we are mainly used to recognize neoplastic tissue as with a parenchymatous-solid pattern and therefore with an iso-hypo T2 signal intensity (T2SI) [3–5], on the contrary we found an impressive percentage of high T2 signal intensity in the familial cancers of our cohort. Over these 43, for 2 lesions the T2weighted sequence was inadequate or not acquired, while 33/41 (80.5%) cancers showed an unusual high T2SI. Over the highT2 neoplasm, 19/33 = 57.5% were BRCA1 related, 27/33 = 82% were Invasive carcinoma, 1 of which with a mucinous subtype. The triple negative status had not been calculated for 5 lesions while 9/28 = 32% were confirmed to be triple negative. For 2 of the 33 neoplasm with high T2SI the grading status was not disposable, but interestingly none of the hyper T2 lesion was tumor grade I, 21/31 = 67.7% were GIII and 10/31 = 32.2% were GII. Conversely, we found 5 GIII neoplasms among the low-middle T2SI neoplasm: 1 DCIS, 1 relapse over the scar of a previous conservative resection and 3 invasive cancers (Table 1).

Over the second branch of the study, 92.5% (37/40) of sporadic cancers had as expected a parenchymatous pattern on T2-weighted images and for the remaining 8% (3/40) 2 were pure Invasive with

* Giovanna Trecate, Unit of Diagnostic Radiology "1", Fondazione IRCCS Istituto Nazionale dei Tumori, via G. Venezian 1, 20133 Milan, Italy. Tel.: +39 0223903689; fax: +39 0223902548.
E-mail addresses: giovanna.trecate@istitutotumori.mi.it (G. Trecate); roberto.agresti@istitutotumori.mi.it (R. Agresti); laura.suman@istitutotumori.mi.it (L. Suman); barbara.valeri@istitutotumori.mi.it (B. Valeri); daniele.vergnaghi@istitutotumori.mi.it (D. Vergnaghi); monica.marchesini@istitutotumori.mi.it (M. Marchesini); claudio.ferranti@istitutotumori.mi.it (C. Ferranti); cristina.ferraris@istitutotumori.mi.it (C. Ferraris); siranoush.manoukian@istitutotumori.mi.it (S. Manoukian); gianfranco.scaperotta@istitutotumori.mi.it (G. Scaperrotta); sara.vigano@istitutotumori.mi.it (S. Viganò); pietro.panizza@istitutotumori.mi.it (P. Panizza).

Table 1
Magnetic resonance morpho-kinetic phenotype in hereditary breast cancers

Pt	Morphological characteristics	Margins	Internal enhancement	Location	Dynamic Curve	T2SI	Histology	Grading	BRCA	ER, PgR, p158 (Her2neu)
1	Oval mass-like enhancement	Irregular	Homogeneous	Central quadrant prepectoral	Wash out	Very high	IDC	G3	BRCA1	ER–PgR–p185 0
2	Round mass-like enhancement	Smooth	Homogeneous	Central quadrant	Plateau	Very high	IDC	G3	BRCA1	ER–PgR–p185 2+
3	Round mass-like enhancement	Smooth	Homogeneous	Lower outer	Plateau	ND	IDC	ND	BRCA1	ER–PgR–p185 3+
4	2004: Round mass-like enhancement (2 contiguous)	Irregular	Rim enhancement	Left upper inner prepectoral	Wash out	Very high	ILC+ LCIS	G3	BRCA2	ER–PgR–p185 2+
4bis	2009: Round mass-like enhancement	Irregular	Rim enhancement	Right upper inner nipple infiltration	Wash out	Very high	IDC	G2		ER+PgR–p185 2+
5	Round mass-like enhancement	Irregular	Homogeneous	Lower outer	Wash out	ND	IDC	G1	HFR	ER+PgR+ p185 ND
6	7–2004: Round mass-like enhancement (some small contiguous)	Irregular	Homogeneous	Upper inner	Wash out	Very high	IDC	G3	BRCA1	ER–PgR–p185 0
	12–2004: Unchanged	Irregular	Homogeneous		Wash out	Very high				
7	Round mass-like enhancement	Smooth	Homogeneous	Central quadrant	Wash out	Very high	IDC + DCIS	G3	BRCA1	ER–PgR–p185 3+
8	3–2008: Dendritic enhancement 10×2 mm	Irregular	Heterogeneous	Upper outer prepectoral	Steady	Medium intensity		G3	BRCA1	ER–PgR–p185 2+
	6–2008: Oval mass-like enhancement (one single) 15 mm	Irregular	Homogeneous		Steady	Medium intensity	DCIS			
9	Oval mass-like enhancement	Smooth	Homogeneous	Central quadrant	Wash out	Very high	IDC	G2	BRCA1	ER–PgR–p185 2+
10	Oval mass-like enhancement (2 contiguous)	Irregular	Homogeneous	Upper inner	Wash out	Low Intensity	IDC	G3	BRCA1	ER–PgR–p185 2+
11	Right: irregular shape (non mass-like)	Irregular	Homogeneous	Upper outer prepectoral	Plateau	Low Intensity	ND	G3	BRCA2	ER+PgR–p185 ND
	Left a) Round mass-like enhancement	Irregular	Rim enhancement	Lower outer	Wash out	Very high	IDC			
	Left b): irregular shape (non mass-like)	Irregular	Homogeneous	Upper outer prepectoral	Wash out	Very high	DCIS			
12	Round mass-like enhancement (many contiguous)	Irregular	Homogeneous	Upper inner	Steady	Medium intensity	IDC	G3	BRCA1	ER–PgR–p185 0
13	RM not performed	-	-	-	-	-	IDC + DCIS		HFR	ER–Pg–p185 3+
14	12–2002: irregular shape (non mass-like)	Irregular	Heterogeneous	Central quadrant	Wash out with delay as lobular type unchanged	Medium intensity	DCIS+ LCIS	G2	HFR	ND
	7–2003: Unchanged	same								
15	Round mass-like enhancement (2 small contiguous)	Smooth	Homogeneous	Upper inner Prepectoral	Plateau	Very high	IDC + DCIS	G3	BRCA1	ER–PgR–p185 0
16	9–2005: Round mass-like small contiguous foci 5×18 mm	Smooth	Homogeneous	Central quadrant	Wash out	Very high				
	12–2005: Irregular Shape (Non mass-like) with several contiguous Dendritic Aspects 18×10 mm	Irregular	Heterogeneous	Central quadrant	Wash out	Very high	IDC + DCIS	G3	BRCA1	ER–PgR–p185 0
17	2–2006: Ductal enhancement 8×2 mm	Irregular	Homogeneous	Central quadrant	Wash out	Low Intensity		G3	BRCA2	ER–PgR–p185 2+
	8–2006: Round mass-like enhancement (some contiguous) 10×4 mm	Irregular	Homogeneous		Wash out	Low Intensity	IDC+ ILC			
18	Round mass-like enhancement	Irregular	Homogeneous	Upper outer	Wash out	Medium intensity	Invasive tubular carcinoma	G1	HFR	ER–PgR–p185 0

continued on next page

Table 1
(*continued*)

Pt	Morphological characteristics	Margins	Internal enhancement	Location	Dynamic Curve	T2SI	Histology	Grading	BRCA	ER, PgR, p158 (Her2neu)
19	6–2007: Round mass-like enhancement 6 mm	Smooth	Homogeneous	Upper outer	Steady	Very high	Invasive carcinoma	ND	BRCA1	ER-PgR-p185 0
	10–2007: Oval mass-like enhancement 14 mm	Irregular	Rim enhancement	Posterior portion of the breast	Steady	Very high				
20	Round mass-like enhancement	Smooth	Homogeneous	Upper outer prepectoral	Wash out	Medium intensity	IDC + DCIS	G3	BRCA1	ER–PgR–p185 0
21	Oval mass-like enhancement	Irregular	Rim enhancement	Upper outer prepectoral	Steady	Medium intensity	IDC + LCIS	G3	BRCA1	ER–PgR–p185 0
22	Round mass-like enhancement	Irregular	Rim enhancement	Upper inner posterior portion of the breast	Plateau	Very high	IDC + DCIS	G3	BRCA2	ER–PgR–p185 3+
23	6–2009: Round mass-like enhancement 11×13 mm	Irregular	Homogeneous	Central quadrant prepectoral	Wash out	Very high	IDC	G3	BRCA1	ER+PgR+p185 1+
	9–2009: Round mass-like enhancement 15×20 mm associated to two more	Irregular	Homogeneous	Prepectoral	Steady	Very high	IDC			
	Round mass-like enhancement of 7 and 6 mm	Irregular	Homogeneous	Prepectoral						
24	11–2005: Dendritic enhancement 5×18 mm	Irregular	Heterogeneous	Central quadrant	Plateau	Very high		G3	BRCA1	
	11–2006: Round mass-like enhancement 12×18 mm	Irregular	Rim enhancement	same	Plateau	Very high	IDC			ND
25	3–2006: Oval mass-like enhancement (some small contiguous)	Smooth	Homogeneous	Upper outer	Wash out	Very high	DCIS + LCIS	G2	BRCA2	ER–PgR–p185 3+
	7–2006: Unchanged	same	same	same	Wash out	Very high				
26	Round mass-like enhancement	Irregular	Rim enhancement	Upper outer prepectoral	Wash out	Very high	IDC	G3	BRCA1	ER–PgR–p185 2+
27	Round mass-like enhancement	Smooth	Homogeneous	Central quadrant	Plateau	Very high	IDC	G3	BRCA1	ND
28	Round mass-like enhancement (some contiguous within scar)	Irregular	Heterogeneous	Lower outer prepectoral	Wash out	Very high	IDC + ILC	G2	HFR	ER+PgR–p185 1+
29	11–04: irregular shape (non mass-like)	Irregular	Homogeneous	Upper outer prepectoral	Wash out mixed with Steady	Very high	IDC	G2	HFR	ER+PgR–p185 1+
	3–05: Unchanged	same	same	same	Wash out only	same				
30	11–08 Round mass-like enhancement 8 mm	Smooth	Homogeneous	Upper outer	Steady	Very high	IDC + DCIS	G2	BRCA2	ER+PgR–p185 0
	5–09 Round mass-like enhancement + irregular flare 12 mm	Irregular	Homogeneous		Wash out	Very high				
31	10–08: Round mass-like enhancement (some contiguous) 16 mm	Irregular	Homogeneous	Upper inner	Wash out	Very high	IDC+DCIS	G2	BRCA1	ER+PgR-p185 0
	2–09: Round mass-like enhancement (many contiguous) 33 mm	Irregular	Homogeneous	Upper inner	Wash out	Very high				
32	Round mass-like enhancement	Smooth	Homogeneous	Lower outer	Wash out	Very high	LCIS + ductal hyperplasia with atypical foci	ND	BRCA1	ND
33	Dendritic	Irregular	Heterogeneous	Upper inner	Steady	Very high	IDC	G3	BRCA1	ND
34	Round mass-like enhancement	Smooth	Heterogeneous	Upper outer prepectoral	Wash out	Very high	IDC	G3	BRCA1	ER–PgR–Her2–
35	Dendritic	Irregular	Heterogeneous	Lower outer	Steady	Very high	DCIS	G3	TP53	ND
36	Mass-like	Irregular	Homogeneous	Central quadrant prepectoral	Wash out	Very high	IDC	G3	BRCA1	ER–PgR–Her2–

continued on next page

Table 1
(*continued*)

Pt	Morphological characteristics	Margins	Internal enhancement	Location	Dynamic Curve	T2SI	Histology	Grading	BRCA	ER, PgR, p158 (Her2neu)
37	Lobulated mass-like	Irregular	Heterogeneous	Lower outer	Plateau	Very high	IDC + ILC	G2	BRCA2	ER+PgR+Her2−
38	Mass-like	Irregular	Homogeneous		Plateau	Very high	DCIS	G2	BRCA1	ER+PgR+Her2−
38bis	Dendritic	Irregular	Homogeneous		Plateau	Very high	IDC	G3		ER+PgR+Her2−
39	Mass-like + dendritic	Irregular	Heterogeneous	Upper inner and outer	Steady	Very high	DCIS	G3	HFR	ER+PgR-Her2+
40	Mass-like	Irregular	Heterogeneous	Upper outer	Steady	Very high	IDC	G3	HFR	ER-PgR-Her2+
40bis	Dendritic	Irregular	Heterogeneous	Upper outer	Steady	Very high	DCIS	G2		ER+PgR−Her2−
41	Dendritic	Irregular	Heterogeneous	Upper and lower outer		Very high	IDC	G3	BRCA2	ER−PgR−Her2−

IDC, Invasive ductal carcinoma; DCIS, Ductal carcinoma in situ; ILC, Invasive lobular carcinoma; LCIS, Lobular carcinoma in situ; HFR, High familial risk; ND, Not done.

triple negative status and 1 was IDC+DCIS. No mucinous variant was found in this branch but again interestingly all of them belonged to tumor grading III which is an established indicator of breast cancer outcome (Table 2).

Beside the MRI semeiotic observation, we noticed that the high T2SI especially occurred in malignancies with high speed of growth.

4. Discussion

Several histopathologic components in benign and malignant breast lesions may be at the basis of high signal intensity on T2-weighted magnetic resonance imaging. The interesting finding of our experience is the significantly high proportion of high T2SI in mutation related cancers. Some authors [4,5] describe how HighT2SI is typically associated with cysts, fibroadenomas, mucinous carcinomas and therefore it usually evokes a liquid or lapse matrix. Yuen and colleagues [4] explain how in nonmucinous carcinomas, T2SI may be attributed to a mixture of some biological backgrounds as a higher proportion of cells than stroma, abundant cytoplasma, edematous stroma, and hemorrhage. Moreover Santamaria and colleagues [5] describe how both benign and malignant tumors may exhibit highT2SI depending on their inner structure. Histopathologic features at the basis of this phenomenon include cystic or sebaceous components, mucinous stroma, loose myxoid stroma, stromal edema, hemorrhagic changes or necrosis and they underline how extensive necrosis (high T2SI) within an invasive carcinoma may be indicative of a rapid growth rate and unfavourable prognosis. Even early rim enhancement observed on MRI images may reflect some histologic features of angiogenesis or a structure where viable cells are located at the periphery, where positive VEGF expression correlated significantly [6]. Uematsu and colleagues [7] show how triple negative cancers often are a smooth mass border with high intratumoral T2SI. Jones and colleagues [8] describe high-grade invasive ductal carcinomas with a large central acellular zone and aggressive biologic behaviour and pointed out their resemblance to tumor with germ-line BRCA1mutation. What we observed in our experience is: the high frequency of highT2SI in hereditary neoplasm (Figs. 1,2) – even without internal necrosis- and the correlation between the highT2SI with the high speed of growth of these neoplasms (Fig. 3). It seems therefore reasonable to suppose that this almost characteristic T2SI reflects a specific histological matrix in familial breast cancers. Interestingly Jones and colleagues [8] describe how the lack of cells in the inner part of those high grade carcinoma with likeness to BRCA1 germ-line corresponds to a major collagen component, necrosis, tissue infarction. All of these biological components can explain the raise of T2SI which should therefore became a semeiotic marker of high

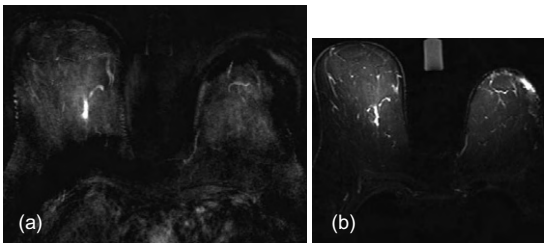

Fig. 1. (a) Non mass, ductal enhancement in the upper right quadrant of the right breast in a BRCA1 mutated patient corresponding to a IDC. (b) The T2SI is very high, equal to the one of vessels.

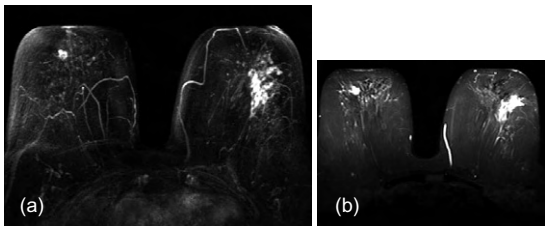

Fig. 2. (a) Non mass, ductal and dendritic enhancement in the left breast, detected during preoperative evaluation for a mucinous carcinoma of the right breast. (b) As expected, the T2SI is very high for the mucinous variant, but also for the dendritic controlateral features. The patient belonged to the HR group. Histology revealed extensive DCIS on the left.

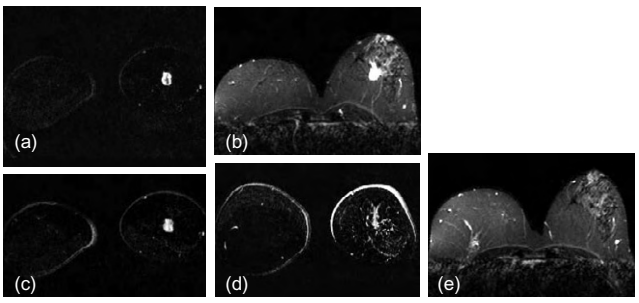

Fig. 3. High T2SI seems to follow the aggressiveness of breast cancer. (a) Rim enhancement considered as indicative of more aggressive behaviour with corresponding very high T2SI (b) in a BRCA1 mutated patient. (c) Notice the complete internal enhancement of the lesion on the last subtracted images which attest the absence of necrosis. (d) One year before, tiny, not convincing enhancement because of artefact motion, with negative findings at Mammography and Ultrasound. The corresponding T2SI at this time is completely silent (e).

Table 2
Magnetic resonance morpho-kinetic phenotype in sporadic cancers

Pt	Morphological characteristics		Margins	Internal enhancement	Dynamic curve	T2SI[a]	Histology	Grading	Receptors
	MLE	NML							
1	Mass-like lobulated		Irregular	Heterogeneous	Steady	0	ILC	G1	E+P+Her2−
2	Mass-like Oval		Irregular	Heterogeneous	Steady	0	ICnos	G2	E+P+Her2−
3		Segmental	Irregular	Heterogeneous	Steady	0	IDC	G2	E+P+Her2−
4		Dendritic	Irregular	Heterogeneous	Plateau	0	ILC	G2	E+P+Her2−
5	Mass-like lobulated		Irregular	Heterogeneous	Wash-out	1	IDC + ILC	G2	E+P+Her2−
6		Segmental	Irregular	Heterogeneous	Plateau	0	IDC	G2	E+P+Her2−
7	Mass-like round		Irregular	Heterogeneous	Wash-out	1	IDC	G2	E+P+Her2−
8	Several round		Regular	Homogeneous	Wash-out	**0+2**	IDC	**G3**	E+P+Her2−
9	Several round		Irregular	Heterogeneous	Plateau	0	IDC	G2	E+P+Her2+
10	Mass-like oval		Irregular	Heterogeneous	Wash-out	0	ILC	G2	E+P+Her2+
11	Mass-like		Irregular	Heterogeneous	Not available	0	ILC	G2	E+P+Her2−
12	Mass-like round		Regular	Rim	Plateau	0+2	IDC	**G3**	E+P+Her2−
13	Several round		Irregular	Heterogeneous	Wash-out	1	IDC	G1	E+P+Her2+
14	Mass-like round		Irregular	Homogeneous	Not available	0+2	IDC	**G3**	E+P+Her2−
15	Mass-like		Irregular	Heterogeneous	Plateau	0+2	IDC	**G3**	E+P+Her2+
16		Dendritic	Irregular	Heterogeneous	Wash-out	**1**	IDC	**G3**	E+P+Her2−
17		Dendritic	Irregular	Heterogeneous	Steady	**2**	IDC	**G3**	E+P+Her2−
18	Mass-like round		Irregular	Heterogeneous	Wash-out	**2**	IDC	**G3**	E−P−Her2−
19	Mass-like round		Irregular	Rim	Plateau	1	IDC	G2	E+P+Her2−
20	Several round		Irregular	Heterogeneous	Steady	0	ILC	G2	E+P+Her2−
21		Dendritic	Irregular	Heterogeneous	Wash-out	1**+2**	ILC	**G3**	E+P+Her2−
22	Mass-like oval		Irregular	Heterogeneous	Steady	0	IDC	G2	E+P+Her2−
23	Mass-like oval		Irregular	Homogeneous	Plateau	0	IDC + ILC	G2	E+P+Her2−
24		Regional	Irregular	Heterogeneous	Plateau	1**+2**	DCIS comedo	**G3**	E−P−Her2+
25	Mass-like lobulated		Irregular	Heterogeneous	Wash-out	1	IDC	G2	Not available
26		Segmental	Irregular	Heterogeneous	Wash-out	0	IDC	G2	E+P>10 e <33% Her2−
27	Mass-like oval		Irregular	Heterogeneous	Plateau	0	IDC	G2	E+P+Her2−
28	Mass-like		Irregular	Rim	Wash-out	**2**	IDC	**G3**	E−P−Her2−
29		Segmental	Irregular	Heterogeneous	Wash-out	0	ILC	G2	Not available
30	Mass-like round		Irregular	Rim	Steady	0	ILC	G2	E+P−Her2−
31	Mass-like round		Irregular	Heterogeneous	Wash-out	**0+2**	IDC	**G3**	E+P>33% e <66%Her2−
32	Mass-like round		Irregular	Rim	Wash-out	0	IDC + DCIS	G2	E+P+Her2−
33	Mass-like round		Irregular	Homogeneous	Wash-out	1	IDC + DCIS	G2	E+P+Her2−
34		Dendritic	Irregular	Heterogeneous	Wash-out	0	DCIS	G2	E+P+Her2−
35	Mass-like round		Irregular	Heterogeneous	Plateau	0	IDC	G2	E+P+Her2−
36		Dendritic	Irregular	Heterogeneous	Steady	0	ILC	G2	E+P−Her2−
37		Segmental	Irregular	Heterogeneous	Wash-out	0	ILC	G2	E+P−Her2−
38		Segmental	Irregular	Heterogeneous	Steady	0	IDC + DCIS	G2	E+P+Her2−
39	Mass-like round		Irregular	Heterogeneous	Wash-out	0/1	IDC + ILC	G2	E−P−Her2−
40		Segmental	Irregular	Heterogeneous	Steady	0	DCIS	G2	E+P+Her2−

IDC, Invasive ductal carcinoma; DCIS, Ductal carcinoma in situ; ILC, Invasive lobular carcinoma.

[a] **+2**: Considering the branch of sporadic cancer, all hyper T2 lesions were graded III. For the remaining grading III of the group previously scheduled as iso-hypo intense T2SI (1 or 0), a new assessment of the images showed how, despite the main iso-hypo T2SI of the carcinomas, some small hyper T2 components were detectable (+2).

aggressiveness. This consideration seems to be confirmed by the high percentage of tumor grading II and III of our experience.

The relationship between T2SI and a specific histological matrix in hereditary breast cancers deserves more investigations with particular care to the possible correlation between the SI and the possible biological markers which are responsible of an higher aggressiveness.

Considering the branch of sporadic cancer, all the hyper T2 lesions resulted to be grading III. For the remaining grading III of the group previously scheduled as iso-hypo intense T2SI (1 or 2), a new assessment of the images showed how despite the main iso-hypo T2SI of the carcinomas, some small hyper T2 components were detectable *(T2SI =+2)* (Table 2).

5. Conclusions

There is emerging evidence that tumours in BRCA carriers exhibit specific biological features. In our patients, we noted a recurrent MRI phenotype that need special attention in order to avoid misleading reports and delayed diagnosis. The correlation with the high speed of growth in these cancers deserves some considerations. If we consider that tumour size and nodal status represent the most important prognostic factors in breast cancers, we believe in fact that when a suspicious lesion is seen only on MRI, it is advisable to repeat the examination after 2 or 3 months to avoid false positive results but at the same time to prevent rapid spread of the disease. After this period, despite some recent considerations [9], even if the lesion persists un-findable at conventional imaging, it becomes mandatory to achieve its removal.

Competing interests: The authors have no conflict of interest to declare.

References

1. Tilanus-Linthorst M, Verhoog L, Obdeijn IM, et al. A BRCA1/2 mutation, high breast density and prominent pushing margins of a tumor independently contribute to a frequent false-negative mammography. Int J Cancer 2002;102:91–5.
2. Schrading S, Kuhl CK. Mammographic, US, and MR imaging phenotypes of familial breast cancer. Radiology 2008;246:58–70.
3. Ballesio L, Savelli S, Angeletti M, et al. Breast MRI: are T2 IR sequences useful in the evaluation of breast lesions? Eur J Radiol 2009;71:96–101.
4. Yuen S, Uematsu T, Kasami M, et al. Breast carcinomas with strong high-signal intensity on T2-weighted MR images: pathological characteristics and differential diagnosis. J Magn Reson Imaging 2007;25:502–10.
5. Santamaría G, Velasco M, Bargalló X, Caparrós X, Farrús B, Luis Fernández P. Radiologic and pathologic findings in breast tumors with high signal intensity on T2-weighted MR images. Radiographics 2010;30:533–48.
6. Matsubayashi R, Matsuo Y, Edakuni G, Satoh T, Tokunaga O, Kudo S. Breast masses with peripheral rim enhancement on dynamic contrast-enhanced MR images: correlation of MR findings with histologic features and expression of growth factors. Radiology 2000;217:841–8.
7. Uematsu T, Kasami M, Yuen S. Triple-negative breast cancer: correlation between MR imaging and pathologic findings. Radiology 2009;250:638–47.
8. Jones C, Ford E, Gillett C, et al. Molecular cytogenic identification of subgroups of grade III invasive ductal breast carcinomas with different clinical outcomes. Clin Cancer Res 2004;10:5988–97.
9. Elshof LE, Rutgers EJ, Deurloo EE, et al. A practical approach to manage additional lesions at preoperative breast MRI in patients eligible for breast conserving therapy: results. Breast Cancer Res Treat 2010;124(3):707–15.

EPOS™

Electronic Presentation Online System

ECR 2012 – Confirmation of Poster Presentation

This is to officially confirm that

S. Viganò[1], L. M. Sconfienza[1], G. Serafini[2], M. Bandirali[1], F. Lacelli[3], A. Aliprandi[4], F. Sardanelli[5]; [1]San Donato Milanese/IT, [2]Pietra Ligure (SV)/IT, [3]Pietra Ligure/IT, [4]S.Donato Milanese MI/IT, [5]San Donato Milanese, Milan/IT

presented the electronic poster entitled

C-1319 - US-guided percutaneous treatment of calcific tendinitis of the rotator cuff: tips & tricks

10.1594/ecr2012/C-1319

within the scientific and educational programme
at the European Congress of Radiology 2012,
held March 1–5, 2012, in Vienna, Austria.

Prof. Felipe Caseiro-Alves
Chairman of the ECR 2012 Scientific Exhibition

Vienna, March 2012

Neurol Sci (2013) 34:799–800
DOI 10.1007/s10072-012-1136-4

LETTER TO THE EDITOR

A case of Wernicke's encephalopathy due to oesophageal achalasia

Federico Pacei · Stephen Mullin · Chiara Colombo · Sara Viganò · Luciano Bet

Received: 2 February 2012 / Accepted: 5 June 2012 / Published online: 24 June 2012

Dear Editor,

A 60-year-old man was admitted to the Emergency Room because of recurrent episodes of food regurgitation. No history of alcohol or substance abuse was elicited and there was no significant past medical history. Neurological examination was unremarkable. He complained of dysphagia, postprandial vomiting, sialorrhea and weight loss of 10 kg over 5 months. Routine blood chemistry was normal. An oesophagogastroduodenoscopy showed oesophageal achalasia and the patient underwent Heller Myotomy with Dor fundoplication. Two days post-surgery the patient developed a paroxysmal neurological deterioration characterised by severe psychomotor agitation, confusion and delirium with frank visual hallucinations. He was disorientated in time, space, place and person and confabulating. Retrograde, anterograde and semantic memory were severely impaired. He was unable to stand, had marked truncal and limb ataxia and was incontinent of urine and faeces. Deep tendon reflexes were normal in the upper limbs and absent in the lower limbs. There was an almost complete paralysis of the conjugate gaze with overt horizontal nystagmus and miotic, slowly reacting pupils. Cerebrospinal fluid (CSF) analysis revealed an increased cell count (10 cells/cm, all lymphocytes) and a mild increase in CSF protein (75 mg/100 ml). MRI brain showed symmetrical aqueductal, thalamic, mamillary body and quadrigeminal hyperintensity on T2 weighted FLAIR sequences. On DWI ($b = 1{,}000$ s/mm^2), the same areas showed minimal high signal intensities, in particular in the medial thalami). B12 levels were normal. Serum thiamine levels were found to be low (13 nM/l, n.v. 50–200 nM/l) and parenteral thiamine (500 mg three times a day) was administered for 5 days followed by enteral thiamine (250 mg once daily) for 3 months. After 1 week of treatment, the patient became quiet and cooperative but was still disorientated, confabulating and incontinent. Severe retrograde and anterograde memory loss remained as did his visual hallucinations. Horizontal gaze abnormalities and nystagmus gradually improved but ataxia was still present. Repeat CSF analysis was normal. Ten days after the onset of the symptoms an MRI brain demonstrated partial regression of the previous signals abnormalities. By week three ophthalmoplegia and nystagmus had nearly resolved. The extent of confabulations, visual hallucinations and incontinence were markedly improved but were still present. Marked deficits in anterograde memory remained. An brain MRI study performed 4 months later demonstrated near complete resolution of the previously abnormal signal intensities. Following 4 months of intensive neurorehabilitation, the patient is unable to return to work on account of persistent anterograde memory loss and ataxia, however, all other focal

F. Pacei (✉) · L. Bet
Stroke Unit, IRCCS Policlinico San Donato,
San Donato Milanese, Milan, Italy
e-mail: federico.pacei@gmail.com

S. Mullin
Department of Clinical Neurosciences, Royal Free Hospital,
London, UK

C. Colombo
Department of Intensive Care Unit, IRCCS Policlinico
San Donato, San Donato Milanese, Milan, Italy

S. Viganò
Department of Radiology, School of Medicine,
IRCCS Policlinico San Donato, University of Milan,
San Donato Milanese, Milan, Italy

L. Bet
Department of Medical and Surgical Sciences,
School of Medicine, University of Milan,
San Donato Milanese, Milan, Italy

signs have resolved. Wernicke's encephalopathy (WE) is a severe neuropsychiatric disorder caused by a deficiency of thiamine or vitamin B1 [1]. Although commonly associated with withdrawing alcoholics WE can occur in any patient with a history of prolonged malnutrition as well as when there is increased thiamine requirement (as in pregnancy). It has been described following a variety of types of oesophageal and abdominal surgery and is often diagnosed late [1, 2]. Although classically associated with paroxysmal onset ophthalmoplegia, ataxia and confusion only 16–38 % of patients affected by WE present with this triad. It is frequently identified during autopsy and only 20 % of non-alcoholic patients affected by WE are diagnosed before death. Although the diagnosis of WE is clinical, T2 weighted MRI can be useful in it's diagnosis especially in the absence of hard clinical signs; but conversely a normal MR does not rule out WE. Classically high signal is demonstrated symmetrically surrounding the third ventricle, tectal plate and aqueduct with diminished or absent mammillary bodies [3]. These findings correlate with those found post-mortem and may progress to third ventricle and aqueductal atrophy in the weeks following the acute stage of the illness although these changes correlate poorly with progression or resolution of clinical features [4, 5]. The prognosis of WE is highly dependent on the prompt commencement of treatment. Early thiamine administration can reverse the clinical features of the disease, whilst delay may result in severe neurological complications, residual disability and death [1, 3]. Clinicians should have a low threshold for initiating thiamine prophylaxis or treatment in cases where prolonged malnutrition of whatever cause is suspected.

Conflict of interest There are no conflicts of interest to declare.

References

1. Sechi G, Serra A (2007) Wernicke's encephalopathy: new clinical settings and recent advances in diagnosis and management. Lancet Neurol 6(5):442–455
2. Loh Y, Watson WD, Verma A, Chang ST, Stocker DJ, Labutta RJ (2004) Acute Wernicke's encephalopathy following bariatric surgery: clinical course and MRI correlation. Obes Surg 14(1):129–132
3. Galvin R, Bråthen G, Ivashynka A, Hillbom M, Tanasescu R, Leone MA (2010) EFNS guidelines for diagnosis, therapy and prevention of Wernicke encephalopathy. Eur J Neurol 17(12):140818
4. Gallucci M, Bozzao A, Splendiani A, Masciocchi C, Passariello R (1990) Wernicke encephalopathy: MR findings in five patients. AJR Am J Roentgenol 155(6):1309–1314
5. White ML, Zhang Y, Andrew LG, Hadley WL (2005) MR imaging with diffusion-weighted imaging in acute and chronic Wernicke encephalopathy. AJNR Am J Neuroradiol 26(9):2306–2310

European Journal of Radiology 81S1 (2012) S116–S117

Contents lists available at SciVerse ScienceDirect

European Journal of Radiology

journal homepage: www.elsevier.com/locate/ejrad

Screening women at intermediate risk: harm or charm?

Pietro Panizza[a,*], Sara Viganò[b], Luigina Bonelli[c], Massimo Bazzocchi[d], Paolo Belli[e], Massimo Calabrese[c], Davide Caramella[f], Stefano Corcione[g], Alessandro Del Maschio[h], Laura Martincich[i], Stefania Montemezzi[j], Federica Pediconi[k], Antonella Petrillo[l], Francesco Sardanelli[m], Paolo Bruzzi[c]

[a] *Fondazione IRCCS Istituto Nazionale dei Tumori, Milano, Italy*
[b] *Università degli Studi, Postgraduation School in Radiodiagnostics, Milano, Italy*
[c] *IRCCS AOU San Martino – IST, Genova, Italy*
[d] *Università degli Studi, AOU S. Maria della Misericordia, Udine, Italy*
[e] *Università Cattolica del Sacro Cuore, Policlinico "A. Gemelli", Roma, Italy*
[f] *Università degli Studi, Ospedale S. Chiara, Pisa, Italy*
[g] *Az. Ospedaliero Universitaria, Ferrara, Italy*
[h] *Università Vita e Salute, Ospedale San Raffaele, Milano, Italy*
[i] *IRCC, Institute for Cancer Research and Treatment, Candiolo, Torino, Italy*
[j] *AOU Integrata, Ospedale Borgo Trento, Verona, Italy*
[k] *Università La Sapienza, Roma, Italy*
[l] *Istituto Nazionale Tumori IRCCS "G. Pascale", Napoli*
[m] *Università degli Studi, IRCCS Policlinico San Donato, Milano, Italy*

ARTICLE INFO

Keywords:
Breast screening
Breast MRI
Intermediate breast cancer risk
Breast density

Mammography is the proven standard of care for breast cancer screening and has been demonstrated to decrease breast cancer mortality [1]. Nevertheless, the impact of mammographic screening as a prevention tool is not fully satisfactory and breast cancer is still a leading cause of cancer death [2]. This limited efficacy has been attributed both to biological characteristics of breast cancer, sometimes incurable before being detected/detectable, and to the low sensitivity of mammography, which has been shown to miss approximately 50% of breast cancers detected by MRI [3]. Biology and sensitivity are strictly related: for instance, different tests, including MRI [4], may have increased sensitivity toward rapidly growing tumors but maybe they can detect smaller tumors because of their slow growth, potentially leading to overdiagnosis, an emerging problem [5]. As a consequence, any attempt to improve the efficacy of breast cancer screening by increasing sensitivity needs to be carefully evaluated. Besides, sensitivity of mammography is lower in young women and women with dense breast tissue or carrying BRCA mutations [6,7].

These issues led the medical community to search for alternative screening methods, including ultrasonography (US) for young women at moderately increased risk and MRI for high risk women, based on the unproven assumption that any increase in sensitivity would translate in an improvement in efficacy of screening.

With reference to MRI, it has a higher sensitivity compared with mammography alone or combined with US in detecting breast cancer, it is not affected by breast density and was shown to be about twice as sensitive as mammography and/or US [7–13]. Yet, many open questions still remain about MRI as a screening tool, including effect of MRI-based screening protocols on mortality, (potential) long-term adverse effects of yearly contrast-enhanced MRI (implying annual injection of Gd-based contrast material) and overdiagnosis.

In this controversial scenario a multicenter randomized controlled clinical trial has been approved and will be carried out in Italy in order to evaluate MRI performance in terms of sensitivity, specificity, and predictive value in screening of women at intermediate risk of breast cancer. This preliminary, feasibility study aimed to provide information necessary for the design of a large efficacy trial of MRI in screening of women at increased breast cancer risk.

This study is based on a multicenter randomized controlled design comparing two surveillance programs. Women enrolled will be randomly assigned with a 1:1 ratio to yearly two-view mammography and breast US or yearly MRI (only). Recruitment center and age will be the only stratification factors. Considering a mean accrual of 100 cases per years in each centre and participation

* Pietro Panizza, Tel.: +39 0223903804; fax: +39 0223902548.
E-mail address: pietro.panizza@istitutotumori.mi.it (P. Panizza).

of 12 Centres, accrual should be completed within 3 years and this cohort will be available for long-term follow-up and assessments.

Inclusion criteria: women aged 40–59 years with mammographic density based on BI-RADS classification involving more than 75% of the breast area (BI-RADS class 4) and/or cumulative risk at 10 years of at least 5%, or lifetime cumulative breast cancer risk ranging between 15% and 30%. Lifetime cumulative risk will be computed using the IBIS Breast Cancer Risk Evaluation Tool (http://www.ems-trials.org/riskevaluator/). Risk factors not included in IBIS, as birth control pill, tamoxifene use, smoking and alcohol consumption, will be collected.

Exclusion criteria: signs/symptoms of breast cancer; previous diagnosis of ductal carcinoma in situ (DCIS), invasive breast cancer or cancer at any site; BRCA or p53 mutation carrier status; general contraindications to MRI or to administration of contrast agent; ongoing or planned pregnancy (for duration of the study); breast implants.

It has been estimated that 2,400 women should be sufficient for an adequate description of the distribution of risk factors and for projecting the expected number of breast cancer cases in a population comparable with that enrolled in the efficacy trial. The size and duration of the study are obviously inadequate to provide solid evidence on the efficacy of MRI screening on breast cancer mortality and on its long-term adverse effects. Meanwhile, this study will provide valid information not presently available on various aspects of these two surveillance protocols when used in this setting as detection rate, comparative sensitivity, specificity, predictive value and costs. Moreover it will assemble the first cohort of non-negligible size (2,400) of women randomly assigned to MRI versus conventional imaging.

Competing interests: The authors have no conflict of interest to declare.

References

1. Gotzsche PC, Nielsen M. Screening for breast cancer with mammography. Cochrane Database Syst Rev 2011;1:CD001877.
2. Chen J, Pee D, Ayyagari R, et al. Projecting absolute invasive breast cancer risk in white women with a model that includes mammographic density. J Natl Cancer Inst 2006;98:1215–26.
3. Sardanelli F, Podo F. Breast MR imaging in women at high-risk of breast cancer. Is something changing in early breast cancer detection? Eur Radiol 2007;17: 873–87.
4. Furman-Haran E, Schechtman E, Kelcz F, Kirshenbaum K, Degani H. Magnetic resonance imaging reveals functional diversity of the vasculature in benign and malignant breast lesions. Cancer 2005;104:708–18.
5. Woloshin S, Schwartz LM. The benefits and harms of mammography screening: understanding the trade-offs. JAMA 2010;303:164–5.
6. US Preventive Services Task Force. Screening for breast cancer: US Preventive Services Task Force recommendation statement. Ann Intern Med 2009;151:716–726.
7. Kuhl CK, Schrading S, Leutner CC, et al. Mammography, breast ultrasound, and magnetic resonance imaging for surveillance of women at high familial risk for breast cancer. J Clin Oncol 2005;23(33):8469–76.
8. Lord SJ, Lei W, Craft P, et al. A systematic review of the effectiveness of magnetic resonance imaging (MRI) as an addition to mammography and ultrasound in screening young women at high risk of breast cancer. Eur J Cancer 2007;43: 1905–17.
9. Warner E. The role of magnetic resonance imaging in screening women at high risk of breast cancer. Top Magn Reson Imaging 2008;19(3):163–9.
10. Sardanelli F, Podo F, Santoro F, et al.; High Breast Cancer Risk Italian 1 (HIBCRIT-1) Study. Multicenter surveillance of women at high genetic breast cancer risk using mammography, ultrasonography, and contrast-enhanced magnetic resonance imaging (the High Breast Cancer Risk Italian 1 study). Invest Radiol 2011;46(2):94–105.
11. Kuhl C, Weigel S, Schrading S, et al. Prospective multicenter cohort study to refine management recommendations for women at elevated familial risk of breast cancer: the EVA trial. J Clin Oncol 2010;28:1450–7.
12. Sardanelli F, Giuseppetti GM, Panizza P, et al. Sensitivity of MRI versus mammography for detecting foci of multifocal, multicentric breast cancer in fatty and dense breasts using the whole-breast pathologic examination as a gold standard. Am J Roentgenol 2004;183:1149–57.
13. Klijn JG. Early diagnosis of hereditary breast cancer by magnetic resonance imaging: what is realistic? J Clin Oncol 2010;28:1441–5.

Washout of Mass-Like Benign Breast Lesions at Dynamic Magnetic Resonance Imaging

Penampai Tannaphai, MD,† Rubina Manuela Trimboli, MD,‡ Luca Alessandro Carbonaro, MD,* Sara Viganò, MD,‡ Giovanni Di Leo, DrSci,* and Francesco Sardanelli, MD*§*

Objective: This study aimed to estimate the frequency and timing of washout in a series of pathologically proven benign mass-like breast lesions at dynamic magnetic resonance imaging.

Methods: Institutional review board approval was obtained for this retrospective study. We evaluated enhancement kinetics of 33 pathologically confirmed benign breast lesions: fibroadenomas (n = 22), adenosis (n = 6), typical ductal hyperplasia (n = 2), fibroadenoma with ductal hyperplasia (n = 1), fibrosclerosis (n = 1), and inflammatory lesion (n = 1). Coronal 3-dimensional T1-weighted gradient-echo sequences were acquired before/after intravenous injection of 0.1 mmol/ kg gadoterate meglumine (time resolution, 111 seconds), 1 before and 5 after contrast injection. The time point at which the kinetic curve demonstrated a washout was recorded. Cumulative distribution of lesions showing washout was built. Paired comparisons of specificity for washout kinetics were performed using the McNemar test.

Results: Of 33 lesions, washout was never observed in 20 (61%), whereas 13 (39%) showed washout during the study. Of these 13 lesions, only 1 (inflammatory mass) exhibited washout within the first 3 minutes (specificity, 97%), 9 within 6 minutes (specificity, 73%), and 13 within 8 minutes (specificity, 61%). Specificity of washout kinetics within 3 minutes (97%) was significantly larger than that from the sixth minute (73%) and thereafter ($P < 0.016$).

Conclusions: A prolonged observation for dynamic breast magnetic resonance imaging may result in false-positive washout, especially after 6 minutes. Late washout should not be considered a reliable marker of malignancy.

Key Words: magnetic resonance imaging, contrast-enhanced dynamic study, washout kinetics, benign mass-like lesions, fibroadenoma

(*J Comput Assist Tomogr* 2012;36: 301–305)

Magnetic resonance imaging (MRI) of the breast is increasingly used in clinical practice.[1,2] Recently, a multidisciplinary European working group discussed several indications for breast MRI, evaluating a high diagnostic value of this technique for: occult primary breast cancer, screening of high-risk women, suspected breast cancer recurrence (when conventional imaging and needle biopsy are not conclusive), and suspected rupture of a breast implant.[3]

From the *Unità di Radiologia, IRCCS Policlinico San Donato, San Donato Milanese, Milan, Italy; †Department of Radiology, Faculty of Medicine, Ramathibodi Hospital, Mahidol University, Bangkok, Thailand; ‡Scuola di Specializzazione in Radiodiagnostica, Università degli Studi di Milano; and §Dipartimento di Scienze Medico-Chirurgiche, Università degli Studi di Milano, San Donato Milanese, Milan, Italy.

Received for publication November 26, 2011; accepted February 15, 2012.

Reprints: Francesco Sardanelli, MD, Università degli Studi di Milano, Dipartimento di Scienze Medico-chirurgiche, IRCCS Policlinico San Donato, Unità di Radiologia, Piazza E. Malan 2, 20097 San Donato Milanese, Milan, Italy (e-mail: f.sardanelli@grupposandonato.it).

Dr Sardanelli has received research grants from and is a member of the speakers' bureaus for Bracco Group and Bayer Pharma. The other authors report no conflicts of interest.

This role is based on a high diagnostic performance, summarized by the meta-analysis from Peters et al[4] who reported a 90% sensitivity and a 72% specificity for breast MRI. In addition to morphology and enhancement pattern, enhancement kinetics, commonly evaluated by means of region of interest-based curves, also plays an important role in the diagnosis.[5–7] By using kinetic curves alone to differentiate benign from malignant breast lesions, Kuhl et al[8,9] found type 3 (washout) curves in 57% of malignant lesions and only in 6% of benign lesions. The likelihood of breast cancer associated with a washout curve was 87%. Schnall et al[10] reported that 76% of cancers were associated with a washout dynamic curve. Sensitivity and specificity of washout curve alone were reported to be 21% and 90%, respectively, by Bluemke et al.[11] However, Eby et al[12] reported a washout curve in 64 (23%) of 275 BI-RADS 3 lesions with only 1 pathologically proven malignant lesion and the remaining 274 lesions being benign at follow-up.

Thus, emerging questions are as follows: How often do benign lesions show a washout dynamic curve? At which time point is washout visible? The aim of this study was to estimate the frequency and the timing of washout in a series of pathologically proven benign lesions.

MATERIALS AND METHODS

Study Population

Institutional review board approval was obtained for this retrospective study. We reviewed data of 386 breast MR examinations acquired from June 2006 to July 2008. Patients were included in this study if they had at least 1 mass-like lesion confirmed to be benign at histopathology by ultrasound-guided core needle biopsy or vacuum-assisted stereotactic biopsy. Overall, there were 30 patients (29 women and 1 man; age range 19–64 years; mean age [SD], 40 [13] years) with 33 breast lesions.

MRI Protocol and Image Analysis

Breast MRI was performed with a 1.5-T system (Sonata Maestro Class; Siemens Medical Solution, Erlangen, Germany) by using a bilateral dedicated 4-element 2-channel breast coil. The imaging protocol included an axial short tau inversion recovery sequence (repetition time, 5400 milliseconds; echo time, 91 milliseconds; slice thickness, 4 mm; pixel size, 1.4×1.4 mm^2; acquisition time, 6 minutes 52 seconds) and a dynamic study with an intravenous injection of 0.1 mmol/kg gadoterate meglumine (Dotarem, Gd-DOTA; Guerbet, Paris, France), followed by a flush of 20 mL of saline solution at 2 mL/s. The dynamic study involved 1 precontrast acquisition followed by 5 postcontrast acquisitions of coronal T1-weighted 3-dimensional fast low-angle-shot sequences (repetition time, 11 milliseconds; echo time, 4.8 milliseconds; slice thickness, 1.0 mm; pixel size, 1.0×1.0 mm^2; acquisition time, 1 minute 51 seconds).

After the examination, image subtraction was performed as contrast-enhanced minus unenhanced images. Using the first or

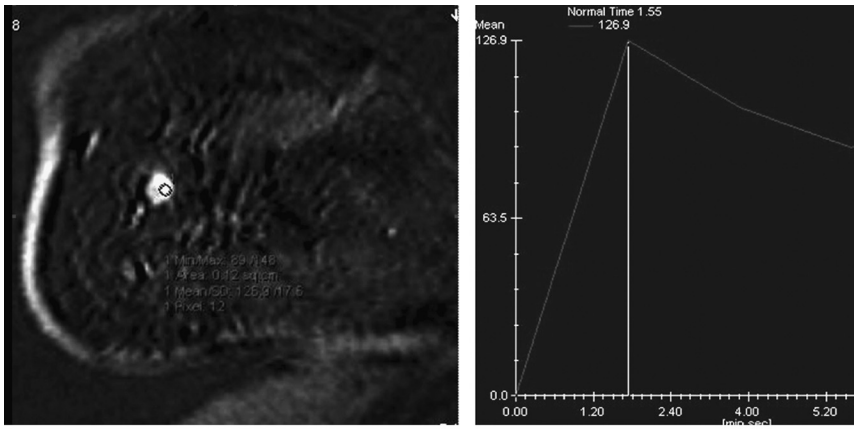

FIGURE 1. A 64-year-old man with a history of mastitis at the right breast with suspicious mass at ultrasound (not shown). A, Coronal contrast-enhanced T1-weighted subtracted image showing a 10-mm lesion at the upper outer quadrant of the right breast. B, Enhancement kinetic curve corresponding to the region of interest (circle) showing a reduction of signal intensity larger than 10% within 3 minutes. Histopathology revealed an inflammatory lesion.

the second subtracted series, curves of percent signal variation versus time were obtained by manually placing a 9- to 12-pixel region of interest on areas of maximal enhancement within the lesion.

All breast lesions were evaluated only for enhancement kinetics according to BI-RADS descriptors.[13] A radiologist with 6 years of experience on breast MRI evaluated all examinations and obtained at least 3 curves per lesion, considering the most suspicious for this analysis. The time point at which the kinetic curve demonstrated a washout (ie, a decrease of the signal intensity larger than 10% compared with its peak value[14]) was recorded. Because of the temporal resolution (1 minute 51 seconds), only 5 time points (corresponding to the 5 postcontrast acquisitions) were interpolated to build the dynamic curve. With reference to the peak value, we extrapolated the time point corresponding to washout and approximated it to the nearest integer minute.

Statistical Analysis

Descriptive statistics of histopathology of breast lesions were given. Cumulative distribution up to the eighth minute was calculated. Paired comparisons of specificity were performed using the McNemar test. Then, 95% confidence intervals (CIs) were calculated according the binomial distribution.

RESULTS

The histopathology of all 33 benign breast lesions included in this study was as follows: fibroadenomas (n = 22), adenosis (n = 6), typical ductal hyperplasia (n = 2), fibroadenoma with ductal hyperplasia (n = 1), fibrosclerosis (n = 1), and inflammatory lesion (n = 1).

Of 33 lesions, 13 (39%) showed washout. After contrast material injection, none of them exhibited washout within the first 3 minutes, except for the inflammatory lesion (specificity, 97%; 95% CI, 84%–100%; Fig. 1). After 6 minutes, 9 of 33 lesions (specificity, 73%; 95% CI, 55%–87%) now exhibited a washout. Such lesions included inflammatory mass (n = 1), fibroadenomas (n = 6), fibroadenoma with ductal hyperplasia (n = 1), and adenosis (n = 1). Examples are shown in Figures 2 and 3. Within 8 minutes, 13 lesions (specificity, 61%; 95% CI, 42%–77%) later exhibited a washout, where these lesions now

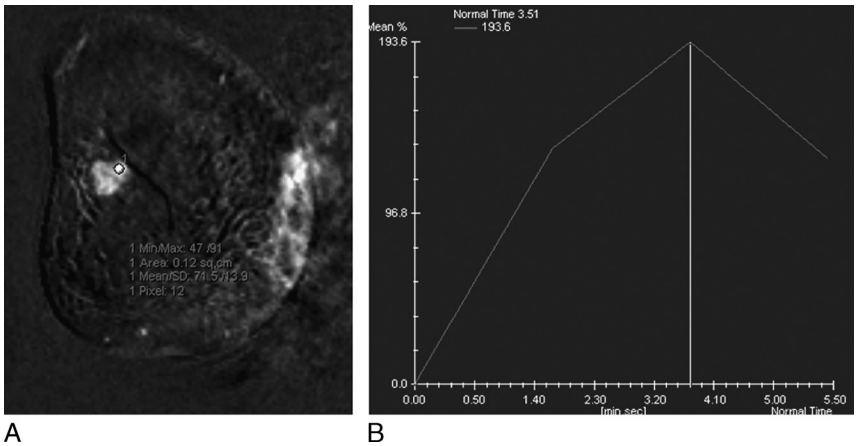

FIGURE 2. A 29-year-old woman with a suspicious mass on the right breast at ultrasound (not shown). A, Coronal contrast-enhanced T1-weighted subtracted image showing a 15-mm well-circumscribed round mass at the upper outer quadrant of the right breast. B, Enhancement kinetic curve corresponding to the region of interest (circle) showing a reduction of signal intensity larger than 10% within 5 minutes. Histopathology revealed a fibroadenoma with ductal hyperplasia without atypia.

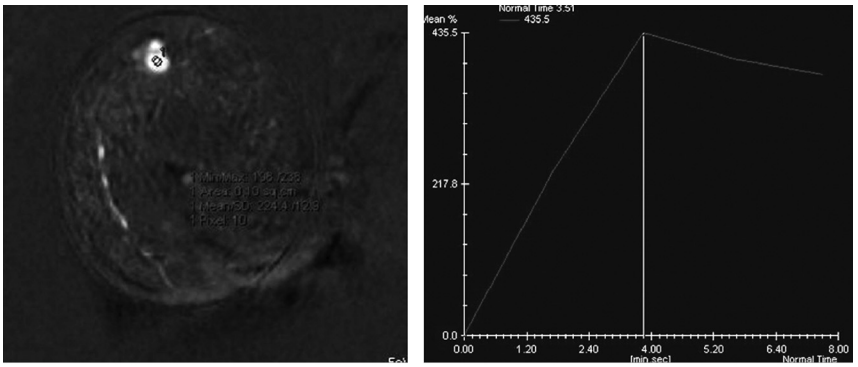

A B

FIGURE 3. A 21-year-old woman with a high family history of breast cancer. A, Coronal contrast-enhanced T1-weighted subtracted image showing a 20-mm well-circumscribed mass at the upper outer quadrant of right breast. B, Enhancement kinetic curve corresponding to the region of interest (circle) showing a reduction of signal intensity larger than10% within 6 minutes. Histopathology revealed a fibroadenoma.

included, in addition to the 9 previously mentioned lesions, 3 fibroadenomas and 1 adenosis (eg, in Fig. 4). Details of histopathology, cumulative percentage of lesions, and specificity are reported in Table 1.

The comparisons of specificity showed that the value obtained at the third minute was significantly larger than that from the sixth minute (73%) and thereafter ($P < 0.016$). The remaining paired comparisons revealed no significant differences.

For the remaining 20 benign breast lesions, the dynamic curve showed no washout up to the eight minute. The histopathology of these lesions was as follows: fibroadenoma (n = 12), adenosis (n = 5), ductal hyperplasia (n = 2), and fibrosclerosis (n = 1).

DISCUSSION

Dynamic contrast-enhanced MRI of the breast has been routinely used to evaluate focal breast lesions. As stated in BI-RADS MRI lexicon 2003,[13] a lesion should be evaluated primarily on the basis of morphology: mass versus non–mass-like enhancement. For non–mass-like enhancement, the diagnosis is based on enhancement pattern rather than kinetic curve.[15,16] To the best of our knowledge, there is no prior study that focused specifically on the timing of washout kinetics in pathologically proven benign lesions. In particular, our question was as follows: if we prolong the acquisition, how many benign lesions do exhibit washout?

In our study, almost 40% (13/33) of the lesions demonstrated a washout curve within 8 minutes; almost 30% (9/33) within 6 minutes. Only 1 lesion, the inflammatory one, showed washout within 3 minutes. The specificity of the washout curve at 3 minutes (97%) was significantly larger ($P < 0.016$) than that from the sixth minute (73%) and thereafter. Within the first 2 minutes, however, none of these benign lesions showed washout.

Because most of the benign lesions in our study were fibroadenomas (66%), we proposed 2 hypotheses, which may explain this delayed washout. First, the native histopathology of young fibroadenomas tends to have rather high microvascular permeability compared with the old fibroadenomas,[17] leading to a high perfusion and diffusion of contrast material to extracellular space and resulting in washout. Nevertheless, because such fibroadenomas do not generate a neovascularization resembling tumor angiogenesis from cancer, the washout curve appeared belatedly. Second, our selected region of interest possibly overlapped with the area of medium caliber vessels along the capsule or septa, resulting in a delayed washout curve,

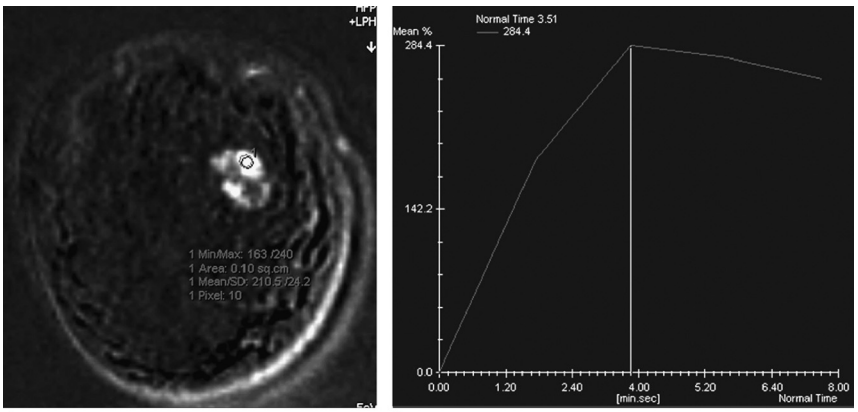

A B

FIGURE 4. A 33-year-old woman with palpable mass at the left breast. A, Coronal contrast-enhanced T1-weighted subtracted image showing a 23-mm inhomogeneous enhancing mass at the upper outer quadrant of left breast. B, Enhancement kinetic curve corresponding to the region of interest (circle) showing a reduction of signal intensity larger than 10% within 8 minutes. Histopathology revealed a fibroadenoma.

TABLE 1. Cumulative Distribution of Lesions Showing Washout

Time Point (Within Minute)	Cumulative Distribution of Lesions Showing Washout	Cumulative Percentage of Lesions Showing Washout†	Histopathology	Specificity (95% CI), %
1	0	0	—	100 (89–100)
2	0	0	—	100 (89–100)
3	1	3	Inflammatory lesion	97 (84–100)*
4	2	6	The previous lesion plus: FA	94 (80–99)
5	5	15	The previous lesions plus: 2 FA, 1 FA with DH	85 (68–95)
6	9	27	The previous lesions plus: 4 FA	73 (55–87)
7	11	33	The previous lesions plus: 1 FA, 1 adenosis	67 (48–82)
8	13	39	The previous lesions plus: 2 FA	61 (42–77)

Specificity was calculated on a total of 33 lesions.

*This value was significantly ($P < 0.016$) larger than all other values obtained from the sixth minute onward.

†This represents the rate of false-positives.

DH indicates ductal hyperplasia; FA, fibroadenoma.

unlike the large neoangiogenesis vessels that showed a rapid washout.[18]

The only lesion demonstrating washout within 3 minutes was an inflammatory mass. It is an expected result. In fact, inflammatory lesions may act like tumor cells in promoting angiogenesis.[19] Fernández-Guinea et al[20] corroborated that peritumor inflammatory lesions were significantly associated with washout.

The study of probably benign lesions from Eby et al[12] reported washout in 23% (64/275) of BI-RADS 3 lesions, a rate not distant from our 30% to 40%. Those 275 lesions were pathologically proven malignant lesions (n = 1) and benign/negative lesions (n = 274). The enhancement features of 64 lesions showing washout were: foci (n = 30), masses (n = 13), and non-mass-like enhancement (n = 21). The only malignant lesion was a 5-mm focus with washout kinetics.

Regarding kinetic curve, we should consider that analysis can be performed with either a qualitative or quantitative method. Kuhl et al[8] described 3 types of time-intensity curves by using qualitative evaluation of the kinetic curve after reaching a peak beyond 2 minutes. This requires experience and is prone to errors especially in deciding whether the curve pattern is a plateau (type 2) or a washout (type 3). Conversely, the quantitative method is easier and more reproducible in the hands of inexpert readers. In this regard, El Khouli et al[21] showed that quantitative assessment of kinetics at breast dynamic contrast-enhanced MRI has significantly higher diagnostic performance than qualitative method. In our study, we used quantitative assessment with 10% minimal reduction for defining washout, as proposed by Fischer et al.[22] They compared the peak percentage of signal intensity within the first 3 minutes to the behavior of the signal intensity curve from the third to the seventh minute. A signal intensity increase of more than 10% within this interval relative to the peak enhancement was defined as "continued signal intensity increase" (giving a type 1 curve). A signal intensity similar to the peak signal intensity was considered as a plateau (giving a type 2 curve), and a decrease of more than 10% was defined as washout (giving a type 3 curve). We adopted this cutoff exploring its effect at the different time points.

According to Kuhl et al,[8] washout should be at any time after 2 minutes from contrast injection, when the change of the shape of the curve is observed visually. However, from the method of Fischer et al, a washout was supposed to be any time from 3 to 7 minutes. When the starting point of reduction in signal intensity for washout curve was considered, our study emphasized that it may be misleading to measure signal intensity decrease after 6 minutes. In fact, the longer we consider, the more false-positive washout occurs. This was demonstrated from specificity: within 3 minutes, it (97%) was significantly larger than that which occurred within 6 minutes (73%) and in later time points ($P < 0.016$).

This study has limitations. First of all, the small number of benign lesions due to the limited number of histopathologically proven benign lesions. Notably, as a rule, we do not use MRI for characterizing equivocal findings at mammography or ultrasound in cases in which a less expensive and more reliable core needle biopsy can be used.[3] Second, we considered for this analysis only the most suspicious of 3 curves, partially simulating what happens in clinical practice, but possibly overestimating the rate of washout. Finally, our MRI technique allowed for a near 2-minute temporal resolution. A better temporal resolution would have permitted more detailed curves but would negatively affected spatial resolution with the hardware and software available in our hands.

In conclusion, approximately 40% of benign lesions showed a washout within 8 minutes. Washout specificity at 3 minutes was significantly larger than that at 6 minutes and thereafter. The prolonged observation may result in false-positive washout, especially after 6 minutes. Timing of washout seems to be crucial to consider it as a reliable marker of malignancy. Using a contrast material, if you have a wash-in, you will always have a washout. It is only a matter of time.

REFERENCES

1. Bassett LW, Dhaliwal SG, Eradat J, et al. National trends and practices in breast MRI. *AJR Am J Roentgenol*. 2008;191:332–339.
2. Mann RM, Kuhl CK, Kinkel K, et al. Breast MRI: guidelines from the European Society of Breast Imaging. *Eur Radiol*. 2008;18:1307–1318.
3. Sardanelli F, Boets C, Borisch B, et al. Magnetic resonance imaging of the breast: recommendations from the EUSOMA working group. *Eur J Cancer*. 2010;46:1296–1316.
4. Peters N, Rinkes I, Zuithoff N, et al. Meta-analysis of MRI imaging in the diagnosis of breast lesions. *Radiology*. 2008;246:116–124.
5. Liberman L, Morris E, Lee M, et al. Breast lesions detected on MR Imaging: features and positive predictive value. *AJR Am J Roentgenol*. 2002;179:171–178.

6. Kinkel K, Helbich T, Esserman L, et al. Dynamic high-spatial-resolution MR imaging of suspicious breast lesions: diagnostic criteria and interobserver variability. *AJR Am J Roentgenol*. 2000;175:35–43.
7. Wiener JI, Schilling KJ, Adami C, et al. Assessment of suspected breast cancer by MRI: a prospective clinical trial using a combined kinetic and morphologic analysis. *AJR Am J Roentgenol*. 2005;184:878–886.
8. Kuhl CK, Bieling HB, Gieseke J, et al. Healthy premenopausal breast parenchyma in dynamic contrast-enhanced MR imaging of the breast: normal contrast medium enhancement and cyclical-phase dependency. *Radiology*. 1997;203:137–144.
9. Kuhl CK, Mielcareck P, Klaschik S, et al. Dynamic breast MR imaging: are signal intensity time course data useful for differential diagnosis of enhancing lesions. *Radiology*. 1999;211:101–110.
10. Schnall MD, Blume J, Bluemke DA, et al. Diagnostic architectural and dynamic features at breast MR imaging: multicenter study. *Radiology*. 2006;238:42–53.
11. Bluemke DA, Gatsonis CA, Chen MH, et al. Magnetic resonance imaging of the breast prior to biopsy. *JAMA*. 2004;292:2735–2742.
12. Eby PR, DeMartini WB, Gutierrez RL, et al. Characteristic of probably benign breast MRI lesions. *AJR Am J Roentgenol*. 2009;193:861–867.
13. American College of Radiology. *ACR Breast Imaging Reporting and Data System (BIRADS): Breast Imaging Atlas*. Reston, VA: American College of Radiology; 2003.
14. Heywang-Kobrunner SH, Beck R. *Contrast Enhanced MRI of the Breast*. 2nd ed. Berlin, Germany: Springer-Verlag; 1996: 7–56.
15. Tozaki M, Fukuda K. High-spatial-resolution MRI of non–mass like breast lesions: interpretation model based on BI-RADS MRI descriptors. *AJR Am J Roentgenol*. 2006;187:330–337.
16. Yabuuchi H, Matsuo Y, Kamitani T, et al. Non–mass-like enhancement on contrast-enhanced breast MR imaging: lesion characterization using combination of dynamic contrast-enhanced and diffusion-weighted MR images. *Eur J Radiol*. 2010;75:126–132.
17. Weinstein D, Strano S, Cohen P, et al. Breast fibroadenoma mapping of pathophysiologic features with three-time-point, contrast-enhanced MR imaging pilot study. *Radiology*. 1999;210:233–240.
18. Sardanelli F, Fausto A, Iozzelli A, et al. Dynamic breast magnetic resonance imaging. Effect of changing the region of interest on early enhancement using 2D and 3D techniques. *J Comput Assist Tomogr*. 2004;28:642–646.
19. Adams TE, Alpert S, Hanahan D. Non-tolerance and autoantibodies to a transgenic self antigen expressed in pancreatic beta cells. *Nature*. 1987;325:223–228.
20. Fernández-Guinea O, Andicoechea A, González LO, et al. Relationship between morphological features and kinetic patterns of enhancement of the dynamic breast magnetic resonance imaging and clinico-pathological and biological factors in invasive breast cancer. *BMC Cancer*. 2010;10:8.
21. El Khouli RH, Macura KJ, Jacobs MA, et al. Dynamic contrast-enhanced MRI of the breast: quantitative method for kinetic curve type assessment. *AJR Am J Roentgenol*. 2009;193:295–300.
22. Fischer U, Vosshenrich R, Döler W, et al. MR imaging–guided breast intervention: experience with two systems. *Radiology*. 1995;195:533–538.

Skeletal Radiol (2013) 42:19–24
DOI 10.1007/s00256-012-1462-x

REVIEW ARTICLE

Double-needle ultrasound-guided percutaneous treatment of rotator cuff calcific tendinitis: tips & tricks

Luca Maria Sconfienza · Sara Viganò · Chiara Martini · Alberto Aliprandi · Pietro Randelli · Giovanni Serafini · Francesco Sardanelli

Received: 16 May 2012 / Revised: 23 May 2012 / Accepted: 27 May 2012 / Published online: 19 June 2012

Abstract Rotator cuff calcific tendinitis is a very common disease and may result in a very painful shoulder. Aetiology of this disease is still poorly understood. When symptoms are mild, this disease may be treated conservatively. Several treatment options have been proposed. Among them, ultrasound-guided procedures have been recently described. All procedures use one or two needles to inject a fluid, to dissolve calcium and to aspirate it. In the present article, we review some tips and tricks that may be useful to improve performance of an ultrasound-guided double-needle procedure.

Keywords Shoulder · Rotator cuff calcific tendinitis · Ultrasound-guided procedures

L. M. Sconfienza (✉) · A. Aliprandi · F. Sardanelli
Servizio di Radiologia, IRCCS Policlinico San Donato,
Via Morandi 30-20097 San Donato Milanese,
Milano, Italy
e-mail: io@lucasconfienza.it

S. Viganò
Scuola di Specializzazione in Radiodiagnostica,
Università degli Studi di Milano,
Via Festa del Perdono 7-20122,
Milano, Italy

C. Martini
Scuola di Specializzazione in Radiodiagnostica,
Università degli Studi di Genova,
Viale Benedetto XV 6,
16132 Genova, Italy

P. Randelli
Unità Operativa di Chirurgia della Spalla,
IRCCS Policlinico San Donato,
Via Morandi 30-20097 San Donato Milanese,
Milano, Italy

P. Randelli · F. Sardanelli
Dipartimento di Scienze Biomediche per la Salute,
Università degli Studi di Milano,
Via Morandi 30-20097 San Donato Milanese,
Milano, Italy

G. Serafini
Servizio di Radiologia, Ospedale Santa Corona,
ASL 2 Savonese, Via XXV Aprile 38-17037 Pietra Ligure,
Savona, Italy

Introduction

Detection of calcifications within the tendons of the rotator cuff is a common occurrence, being found in up to 7.5 % of asymptomatic adults and up to 20 % of painful shoulders. [1–4]. Tiny scattered calcifications may be found on the insertional portion of the tendons as a result of a degenerative process (i.e., calcific enthesopathy). Conversely, rotator cuff calcific tendinitis (RCCT) is a completely different disease, which usually occurs in healthy tendon, as a result of fibrocartilaginous metaplasia of collagen fibroblasts associated with calcium deposition, predominantly hydroxyapatite. This event is probably triggered by oxygen tension decrease and pressure increase within the tendon [2, 3], although etiopathogenesis is still not completely understood. The term *tendinitis* is not really appropriate, as inflammatory cells are rarely encountered [4]. Thus, *calcific tendinopathy* seems to be the most appropriate name for this disease [3]. Two stages of the disease have been recognized: precalcific and calcific. In turn, calcific stage consists of formative, resorptive, and postcalcific phase. Resorptive phase is characterized by vascular invasion, oedema, migration of phagocytic cells, and increased intratendinous pressure. At this time, patients may report the occurrence of highly disabling sharp acute pain, usually scarcely responding

to common painkillers. Occasionally, calcium may drain within the subacromial-subdeltoid bursa (SASD), thus promoting the occurrence of calcium-related bursitis [2, 5].

RCCT is more frequently seen in women in their fourth and fifth decades, and it seems not to be related to physical activity. Theoretically, all tendons of the body may be affected by RCCT, although rotator cuff is by far the most common site. There, the supraspinatus tendon is involved in about two thirds of cases [2, 6].

Notably, RCCT is considered a self-healing condition, with complete *restitutio ad integrum* of tendon matrix and pain regression [3]. However, the temporal self-response of RCCT has been demonstrated to be extremely variable [2, 3]. Being RCCT a self-limiting condition, the chosen treatment should be effective, complication free, and minimally invasive. As far as the treating options are concerned, there are different possibilities, but no standard of care has been established. Nevertheless, no treatment is required for asymptomatic patients, while mild symptoms can benefit from conservative treatments, such as physical therapy and oral non-steroidal anti-inflammatory drugs [5]. Different treatment options have been reported. Iontophoresis has proven not to be more effective than physiotherapy or placebo on long-term follow-up [7]. Shockwave therapy resolves calcifications in 57–60 % of the shoulders and achieves substantial or complete clinical improvement [8]. However, shockwaves are extremely painful when performed during the hyperalgesic crisis [9]; at least three applications are usually needed , and they are relatively expensive [8, 9]. Arthroscopy [10, 11] achieves substantial or complete clinical improvements in 79–100 % of the shoulders, but long rehabilitation is required and even major complications may occasionally occur. Nowadays, it is considered the last option when other methods have failed.

Imaging-guided procedures are considered alternative and effective treatments. Slightly different approaches have been described, performed under fluoroscopic [12] or ultrasound (US) guidance, all implying the use of a fluid (local anesthetic or saline solution) to dissolve calcific deposits. Percutaneous treatment is currently most often performed under US guidance [2, 13–22], thanks to absence of ionizing radiation, three-dimensional capabilities in localizing the calcification, real-time monitoring during needle placement, decreased risk of injury to the neighboring structures, and real time confirmation of procedure success [2]. These procedures are also very quick, having an average duration of 10 to 20 minutes [21]. US-guided percutaneous procedures can be effectively used as first line treatment for RCCT, especially in the acute phase.

US-guided procedures can be performed using one [13, 15, 17, 19] or two needles [2, 14, 16, 18, 20–22] to inject fluid within calcifications. Some authors used one needle, believing that double needle insertion could be harmful to the tendon [25], but safety and efficacy of two-needle technique has been proven up to one and ten years, respectively, and it actually is an effective, quick, and low-cost therapy [2, 21]. Purposes of using two needles are to create a continuous inflow and outflow of saline solution to remove calcium and to control saline pressure inside the calcification during injection [18]. This also provides escape for fluid, avoiding disruption of the peripheral calcific rim that causes calcium to spread throughout the periarticular soft tissues, possibly promoting the occurrence of post-procedural calcific bursitis [2, 21].

The purpose of the present work is to review some tips and tricks based on a daily routine experience that can improve the practical performance of a double-needle procedure for treating RCCT.

Procedure details

US probe disinfection

Preliminary disinfection of instruments is necessary before starting the procedure [6], as US machines are ideal vectors for cross infections [23]. In terms of potential infections, US-guided procedures are argued to be safe for patients and operators with ordinary antisepsis [24]. Although most operators use either sterile gels or liquids in combination with sterile sheaths, condoms or gloves, or non-sterile gel-filled condoms or gloves, this may be an unnecessary procedural effort. Caturelli et al. [25] reported no infection when US transducer was cleaned with a 70 % alcoholic solution prior to each procedure of abdominal fine-needle-puncture of solid organs. To our knowledge, no study is available investigating the infection rate in US-guided joint procedures. When dealing with US-guided percutaneous treatment of RCCT, no infective complications were reported in studies in which the US probe was simply cleaned with antiseptic sterile solution [2, 21]. However, a sterile probe cover can be also used, but it represents an additional cost and may be uncomfortable in a procedure that lasts more than seconds.

Use of a two-step skin cleaning procedure (coloured/uncoloured antiseptics)

We currently use a two-step antiseptic procedure for skin cleaning. It consists of cleaning with a coloured disinfectant (i.e., 7.5–10 % iodopovidone solution) for at least two minutes, immediately followed by a second cleaning with an uncoloured disinfectant (e.g., benzalkonium chloride solution) (Fig. 1). This approach has three practical advantages. First, a two-step procedure improves antisepsis of shoulder skin. Second, using no sterile covers, the US probe is not stained by coloured antiseptic solution. Third, keeping a

Fig. 1 Two-step skin cleaning procedure (coloured/uncoloured antiseptics). The peripheral brownish ring (arrowhead) allows for clear visibility of the cleaned area. The central area is also cleaned with an uncoloured solution, thus avoiding probe staining

peripheral ring of coloured antiseptic solution allows for a better control of the cleaned area during the entire procedure. Thus, not only is the area optimally cleaned, but we are also aware of the external borders of the cleaned area. In case of reported allergy to iodine, we perform a double cleaning with the same uncoloured antiseptic solution reported above [2, 21].

Use of sterile equipment and sterile contact gel

Although this procedure is not usually performed in a surgical theatre, sterility levels should be kept at maximum. Thus, the use of sterile drapes and gloves is advisable [2, 21].

Some authors do not use any sterile contact gels during US-guided procedures [23–25]. This is agreeable, as for short procedures (e.g., injections, biopsies) it is enough to keep both the skin and the probe wet with the antiseptic solution that was used to clean the skin. However, in longer procedures, such as US-guided percutaneous treatment of RCCT, this approach is suboptimal, as the antiseptic solution gets dry quite quickly and it needs to be reapplied frequently. For these reasons, the use of a small amount of sterile lubricant contact gel (e.g., Glissen 12.5 g) may be advisable [2, 21].

How to inject local anaesthesia

Different anaesthetic solutions can be used (e.g., 2 % lidocaine chloridrate). Whatever solution is used, the maximum dose recommended for adults is 400 mg, to be administered during the entire procedure [26]. Anaesthetic solution must be injected mostly (almost two thirds) into the SASD bursa, thus allowing for its complete distension. The remaining solution should be injected in the subcutaneous tissues and around calcification. In order to preserve the peripheral calcific rim, no anesthetic solution should be injected directly within the calcification. No anaesthetic injection is required directly in the deltoid muscle (Fig. 2).

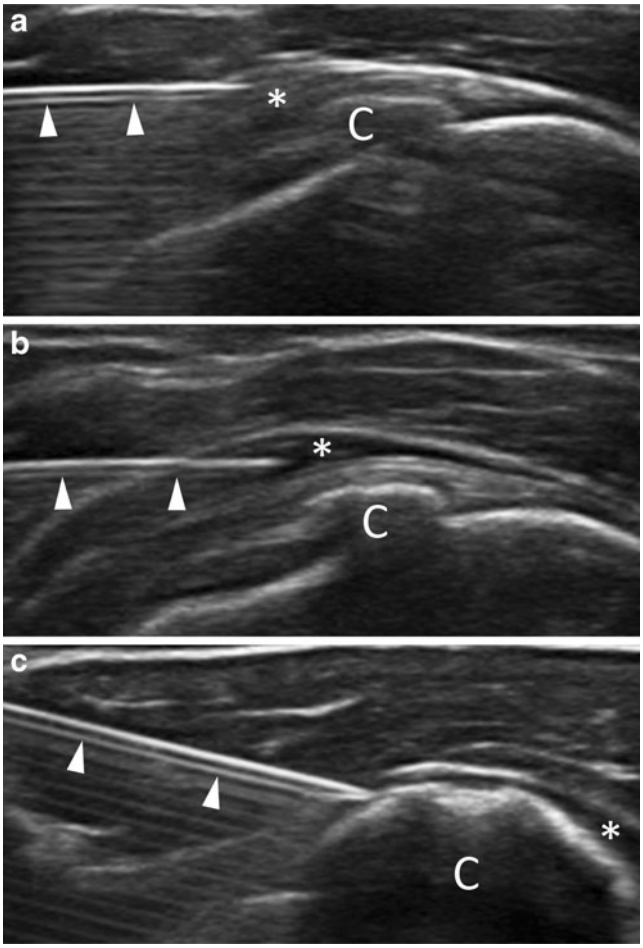

Fig. 2 Anesthetic should be injected (**a**) in the peribursal space, (**b**) within the subacromial subdeltoid bursa (asterisk), and (**c**) around the calcification (C). Arrowheads = needle

How to position the needles

In musculoskeletal procedures, selection of type and size of the needles depends on the joint and on the procedure that is being performed. Drug injection normally needs thin needles of 22–27 gauge (G) [27], while fluid aspiration normally needs thicker needles of 18–21 G. When dealing with RCCT, needle size must be chosen in order to maximize calcium retrieval and avoid obstruction. Aina et al. [15] indicated that 22 G needles are adequate for performing calcification fragmentation, aspiration, and reduction, without the need of larger and more traumatic needle sizes. The caliber of the needles used in other published studies for RCCT treatment varies between 16 and 22 G [13–22]. In our experience [2, 21], using two 16 G needles has been demonstrated to be safe, without risk of tendon tears and a good compromise between calcium retrieval and avoiding obstruction that may occur when thinner needles are used.

Needles are inserted into calcification under continuous US monitoring with a free-hand technique. No needle

guidance kit is required, as freehand technique allows for a faster and more flexible approach (i.e., with no fixed angles) [28].

Correct needle positioning and an adequate visualization of needle tips are crucial [2]. Two aspects must be taken into account: needle positioning with respect to the US probe, and positioning of the two needles with respect to each other and to calcifications.

As far as the position of the needle with respect to the US probe is concerned, methods used to insert the two needles vary according to location, accessibility, and calcification size. Anyhow, both needles must be inserted as parallel as possible to the US probe so they will be as perpendicular as possible to US beam. In this way, anisotropy artefacts are drastically reduced and needles can be seen thoroughly (Fig. 3).

With respect to each other and to calcifications, the deeper needle is first inserted. This prevents the first needle from being covered by the second, which is inserted superficially (Fig. 4). Needles should be placed on a plane so that the US beam can demonstrate both of them and the calcification simultaneously. Angulation between the needles should be 25–30°, with tips very close to each other (maximum distance 2–3 mm). The bevel of the first needle must be rotated upward, while the bevel of the second needle should be rotated downward, so that both bevels are facing each other (Fig. 5). This would allow for facilitating a continuous flow of water that is injected by one needle and drained by the other.

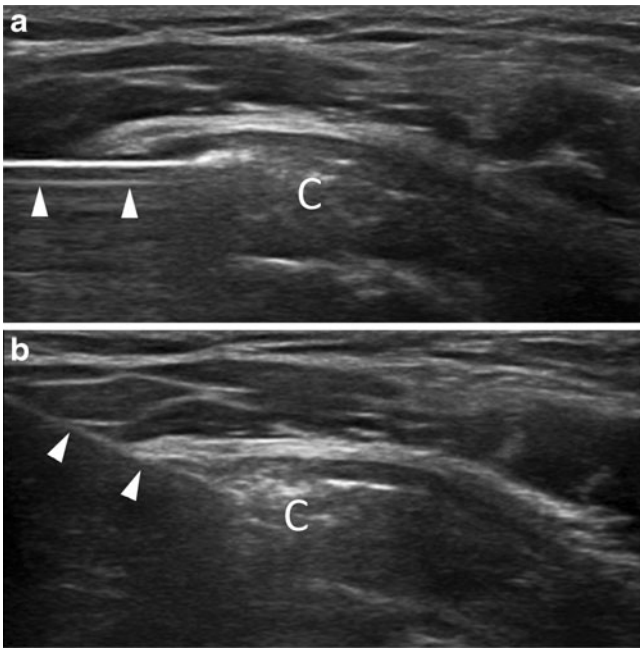

Fig. 3 Positioning of the needles in respect to the probe. The best needle visualization is obtained when (**a**) the needle is as parallel as possible to the US probe, which means as perpendicular as possible to the ultrasound beam. (**b**) As the angle between the beam and the needle decreases, the needle becomes less visible. *C* calcification

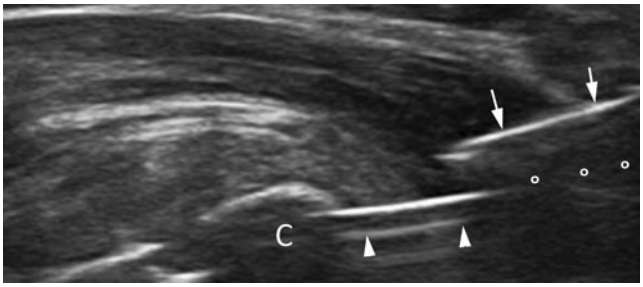

Fig. 4 Needle positioning in respect to each other and to calcification (C). The deep needle (arrowheads) should be inserted first, as its visibility is hindered (circles) by the superficial needle (arrows)

Use of warm saline solution

As mentioned before, all percutaneous treatments for RCCT imply the use of a fluid (saline or anesthetic) to dissolve calcium. Most authors reported the use of room temperature fluid [2, 14–20, 22]. However, we recently demonstrated that use of warm saline solution improves treatment of RCCT [21]. This hypothesis has been tested, starting from the well-known concept that most salts dissolve better in high temperature liquids [29]. Using warm saline solution when treating RCCT allows for significant reduction in procedure duration, compared to the same procedure performed using room temperature saline solution. Using warm saline also improves calcium dissolution and helps in reducing the occurrence of post-procedural bursitis, maintaining a similar efficacy of the treatment.

Saline solution injection

Saline solution is normally injected using a 20-mL syringe. It is connected to one of the needles, and the plunger is repeatedly pushed. Once calcification starts to dissolve, water and calcium debris are drained from the free needle (Fig. 6a). Another option is to build a homemade lavage

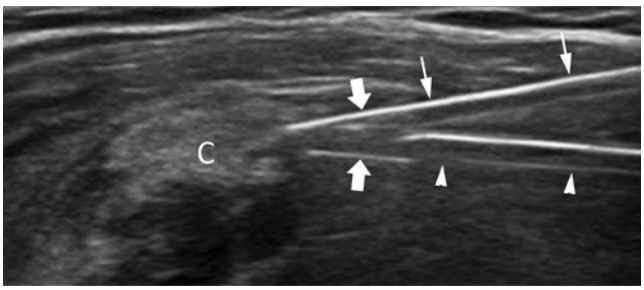

Fig. 5 Needles should be inserted in the same coronal plane, such that they form a maximum angle of 25–30° and their tips are very close to each other (maximum distance 2–3 mm). Deep needle (arrowheads) bevel (thick arrow) must be rotated upward and superficial needle (thin arrows) bevel (thick arrow) should be rotated downward so that they face each other. *C* calcification

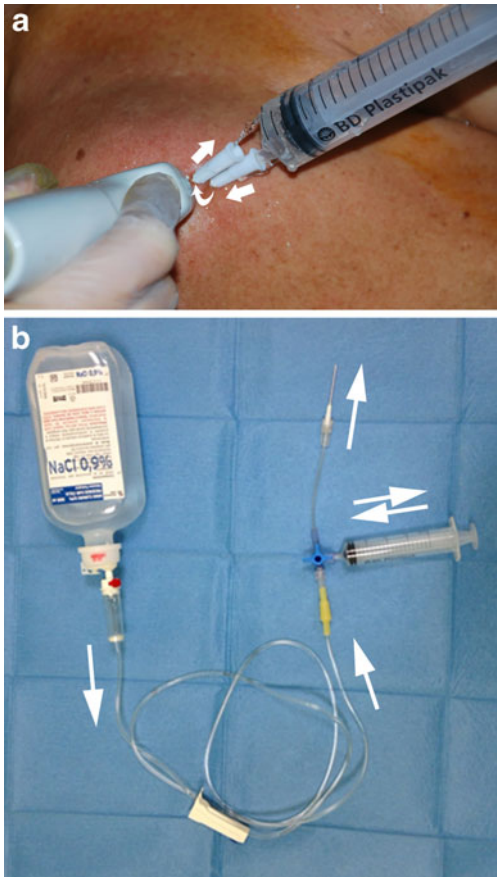

Fig. 6 (**a**) The syringe is connected to one needle. Then, saline solution is injected and flows out through the other needle, thus obtaining a continuous inflow and outflow. (**b**) A home-made close circuit can be also set up. Arrows indicate water flow direction

closed circuit. A saline bottle is hung on a phleboclysis rod and is connected directly to one of the needles using a long tube. A three-way stopcock connected to a syringe is inserted in the line, thus allowing a continuous aspiration and injection of saline within the calcification (Fig. 6b). Although slightly more complicated, this system ensures complete sterility of the procedure [14].

How to increase calcium removal

It is not clear whether there is a correlation between removal of a large amount of calcium and a good outcome, as some studies report satisfactory results, with minimal calcium retrieval [12, 15, 17]. However, removing a large amount of calcium may reduce the occurrence of post-procedural bursitis induced by calcium debris that spreads around the cuff. Although the double-needle technique allows for optimal calcium removal in most cases, hard calcifications are occasionally difficult to melt. In these cases, needles can be gently rotated and laterally displaced (Fig. 7) to increase calcium disaggregation and fragmentation.

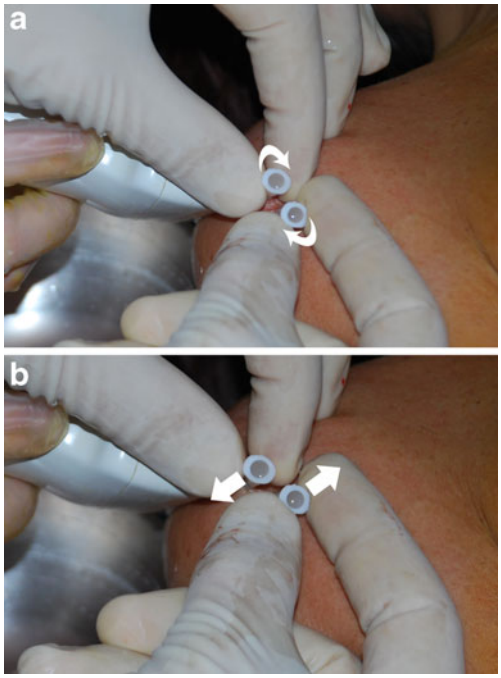

Fig. 7 To improve calcium removal, needles can be gently (**a**) rotated and (**b**) displaced while still inside the calcification

This usually results in easier and more effective calcium washing (Fig. 8). These manoeuvres are performed carefully, trying not to disrupt the peripheral calcific rim.

Conclusion

Double-needle US-guided percutaneous treatment of RCCT has been demonstrated to be an effective, quick, minimally invasive and low-cost therapy. It facilitates shoulder function improvement and prompt pain relief, and post-procedural complications are almost absent. The use of the tips and tricks

Fig. 8 Procedure conclusion. Lavage water and retrieved calcium (whitish material) are collected within an inox bowl

discussed in the present article may further improve the execution of this procedure in the daily practice.

Conflict of Interest Authors have no conflict of interest to disclose.

References

1. Speed CA, Hazelman BL. Calcific tendinitis of the shoulder. N Engl J Med. 1999;340:1582–4.
2. Serafini G, Sconfienza LM, Lacelli F, Silvestri E, Aliprandi A, Sardanelli F. Rotator cuff calcific tendonitis: short-term and 10-year outcomes after two-needle us-guided percutaneous treatment–nonrandomized controlled trial. Radiology. 2009;252:157–64.
3. Uhthoff HK, Sarkar K. Calcifying tendinitis. Baillieres Clin Rheumatol. 1989;3:567–81.
4. Sharma P, Maffulli N. Tendon injury and tendinopathy: healing and repair. J Bone Joint Surg Am. 2005;87:187–202.
5. Bianchi S, Martinoli C, Shoulder in Bianchi S, Martinoli C, eds. Ultrasound of the musculoskeletal system, Berlin, Germany: Springer-Verlag, 2007;190–331
6. Hamada J, Ono W, Tamai K, Saotome K, Hoshino T. Analysis of calcium deposits in calcific periarthritis. J Rheumatol. 2001;28:809–13.
7. Leduc BE, Caya J, Tremblay S, Bureau NJ, Dumont M. Treatment of calcifying tendinitis of the shoulder by acetic acid iontophoresis: a double-blind randomized controlled trial. Phys Med Rehabil. 2003;84:1523–7.
8. Ebenbichler G. Ultrasound therapy for calcific tendinitis of the shoulder. N Engl J Med. 1999;340:1582–4.
9. Mouzopoulos G, Stamatakos M, Mouzopoulos D, Tzurbakis M. Extracorporeal shock wave treatment for shoulder calcific tendonitis: a systematic review. Skeletal Radiol. 2007;36:803–11.
10. Wittenberg RH. Surgical or conservative treatment for chronic rotator cuff calcifying tendinitis—a matched-pair analysis of 100 patients. Arch Orthop Trauma Surg. 2001;121:56–9.
11. Rubenthaler F. Prospective randomized surgical treatments for calcifying tendinopathy. Clin Orthop Relat Res. 2003;410:278–84.
12. Comfort TH, Arafiles RP. Barbotage of the shoulder with image-intensified fluoroscopic control of needle placement for calcific tendinitis. Clin Orthop Relat Res. 1978;135:171–8.
13. Bradley M, Bhamra MS, Robson MJ. Ultrasound guided aspiration of symptomatic supraspinatus calcific deposits. Br J Radiol. 1995;68:716–9.
14. Galletti S, Magnani M, Rotini R, et al. The echo-guided treatment of calcific tendinitis of the shoulder. Chir Organi Mov. 2004;89:319–23.
15. Aina R, Cardinal E, Bureau NJ, Aubin B, Brassard P. Calcific shoulder tendinitis: treatment with modified US-guided fine-needle method. Radiology. 2001;221:455–61.
16. Farin PU, Rasanen H, Jaroma H, Harju A. Rotator cuff calcifications: treatment with ultrasound-guided percutaneous needle aspiration and lavage. Skeletal Radiol. 1996;25:551–4.
17. del Cura JL, Torre I, Zabala R. Legórburu A Sonographically guided percutaneous needle lavage in calcific tendinitis of the shoulder: short- and long-term results. AJR Am J Roentgenol. 2007;189:W128–34.
18. Sconfienza LM, Serafini G, Sardanelli F. Treatment of calcific tendinitis of the rotator cuff by ultrasound-guided single-needle lavage technique. AJR Am J Roentgenol. 2011;197:W366.
19. Giacomoni P, Siliotto R. Echo-guided percutaneous treatment of chronic calcific tendinitis of the shoulder. Radiol Med (Torino). 1999;98:386–90.
20. Farin PU, Jaroma HJ. Sonographic findings of rotator cuff calcifications. J Ultrasound Med. 1995;14:7–14.
21. Sconfienza LM, Bandirali M, Serafini G, et al. Rotator Cuff Calcific Tendinitis: Does Warm Saline Solution Improve the Short-term Outcome of Double-Needle US-guided Treatment? Radiology. 2012;262:560–6.
22. De Zordo T, Ahmad N, Ødegaard F, et al. US-guided therapy of calcific tendinopathy: clinical and radiological outcome assessment in shoulder and non-shoulder tendons. Ultraschall Med. 2011;32:S117–23.
23. Fowler C, McCracken D. US probes—Risk of cross infection and ways to reduce it—Comparison of cleaning methods. Radiology. 1999;213:299–300.
24. Weidner S, Kellner W, Kellner H. Interventional radiology and the musculoskeletal system. Best Pract Res Clin Rheumatol. 2004;18:945–56.
25. Caturelli E, Giacobbe A, Facciorusso D, et al. Free-hand technique with ordinary antisepsis in abdominal US-guided fine-needle punctures: three-year experience. Radiology. 1996;199:721–3.
26. Niesel HC. Local anesthetics: maximum recommended doses. Anaesthesiol Reanim. 1997;22:60–2.
27. De Smet AA. Ultrasound-guided injections and aspirations of the extremities. Semin Roentgenol. 2004;39:145–54.
28. del Cura JL. Ultrasound-guided therapeutic procedures in the musculoskeletal system. Curr Probl Diagn Radiol. 2008;37:203–18.
29. Wiberg E, Wiberg N, Holleman AF. Inorganic chemistry. London, England: Academic Press; 2001. p. 810–1.